



# HHS Public Access

Author manuscript

*Nat Immunol.* Author manuscript; available in PMC 2020 February 19.

Published in final edited form as:

*Nat Immunol.* 2019 September ; 20(9): 1138–1149. doi:10.1038/s41590-019-0467-1.

## IL-1R3 blockade broadly attenuates the functions of six members of the IL-1 family, revealing their contribution to models of disease

Jesper Falkesgaard Højen<sup>1,2,3</sup>, Marie Louise Vindvad Kristensen<sup>3</sup>, Amy S. McKee<sup>3,4</sup>, Megan Taylor Wade<sup>3</sup>, Tania Azam<sup>3</sup>, Lars P. Lunding<sup>5</sup>, Dennis M. de Graaf<sup>3,6</sup>, Benjamin J. Swartzwelter<sup>3</sup>, Michael Wegmann<sup>5</sup>, Martin Tolstrup<sup>1,2</sup>, Karsten Beckman<sup>7</sup>, Mayumi Fujita<sup>4,8</sup>, Stephan Fischer<sup>7</sup>, Charles A. Dinarello<sup>3,6,\*</sup>

<sup>1</sup>Department of Infectious Diseases, Aarhus University Hospital, Aarhus, Denmark. <sup>2</sup>Department of Clinical Medicine, Aarhus University, Aarhus, Denmark. <sup>3</sup>Department of Medicine, University of Colorado Denver, Aurora, USA. <sup>4</sup>Department of Microbiology and Immunology, University of Colorado Denver, Aurora, USA. <sup>5</sup>Division of Asthma Exacerbation & Regulation, Priority Area Asthma and Allergy, Leibniz Lung Center Borstel, Airway Research Center North (ARCN), Member of the German Center for Lung Research (DZL), Borstel, Germany. <sup>6</sup>Department of Internal Medicine, Radboud University Medical Center, Nijmegen, The Netherlands. <sup>7</sup>MAB Discovery GmbH, Neuried, Germany. <sup>8</sup>Department of Dermatology, University of Colorado Denver, Aurora, USA.

### Abstract

IL-1R3 is the co-receptor in three signaling pathways that involve six cytokines of the IL-1 family (IL-1 $\alpha$ , IL-1 $\beta$ , IL-33, IL-36 $\alpha$ , IL-36 $\beta$  and IL-36 $\gamma$ ). In many diseases, multiple cytokines contribute to disease pathogenesis. For example, in asthma, both IL-33 and IL-1 are of major importance, as are IL-36 and IL-1 in psoriasis. We developed a blocking monoclonal antibody (mAb) to human IL-1R3 (MAB-hR3) and demonstrate here that this antibody specifically inhibits signaling via IL-1, IL-33 and IL-36 in vitro. Also, in three distinct in vivo models of disease - crystal-induced peritonitis, allergic airway inflammation and psoriasis, we found that targeting IL-1R3 with a single mAb to mouse IL-1R3 (MAB-mR3) significantly attenuated heterogeneous cytokine-driven inflammation and disease severity. We conclude that in diseases driven by

---

Users may view, print, copy, and download text and data-mine the content in such documents, for the purposes of academic research, subject always to the full Conditions of use:[http://www.nature.com/authors/editorial\\_policies/license.html#terms](http://www.nature.com/authors/editorial_policies/license.html#terms)

\*Corresponding author: Charles A. Dinarello, [cdinare333@aol.com](mailto:cdinare333@aol.com).

#### Author contributions

J.F.H. designed and performed experiments, analyzed data and wrote the manuscript. M.L.V.K. designed and performed experiments and analyzed data and assisted with manuscript preparation. A.S.M. and M.T.W. designed and performed experiments and analyzed data. T.A., L.P.L., D.M.D.G., B.J.S. and M.W. performed experiments and analyzed data. M.T. assisted in the experimental design and manuscript preparation. K.B. designed experiments and analyzed data. M.F. designed and supervised experiments and analyzed data. S.F. produced the human and mouse anti-IL-1R3 antibodies, designed experiments and analyzed data. C.A.D. designed experiments, analyzed data and edited the manuscript. All authors have read and accepted the final manuscript.

#### Competing financial interests

K.B. is employed by and S.F. is the CEO of MAB Discovery GmbH, Neuried, Germany. All other authors declare no conflicts of interest.

multiple cytokines, a single antagonistic agent such as a mAb to IL-1R3 is a novel therapeutic option with considerable translational benefit.

Inhibition of cytokine function is a cornerstone of many clinical interventions. Although treatment often focuses on blocking either a single ligand or its primary receptor<sup>1</sup>, targeting a single cytokine can imply that a disease is due to a distinct mediator. However, this is not always the case. The heterogeneous nature of inflammatory diseases may explain less than optimal outcomes or failures in clinical trials when neutralizing only a single cytokine. In particular, when preclinical models reveal synergy of two cytokines. Diseases where more than one IL-1 family member has been attributed a prominent role, such as IL-1 $\beta$  and IL-33 in asthma<sup>2, 3</sup> and IL-1 $\alpha$  and IL-36 in psoriasis<sup>4, 5</sup>, emphasizes this heterogeneity. Since there is a basal inflammatory component in most diseases, blockade of the specific disease-driving cytokine as well as the inflammatory component would therefore likely improve outcomes.

The IL-1 family is comprised of 11 members, with a role in innate inflammation and acquired immunity<sup>6</sup>. In search for an improved druggable target in the IL-1 family, we assessed possible interventional sites. The receptor family is comprised of 10 members and one binding protein (IL-18BP)<sup>7</sup>. Of these, IL-1R1 binds IL-1 $\alpha$  and IL-1 $\beta$  recruiting IL-1R3 to form the trimeric signaling complex. IL-1R4 (ST2) binds IL-33 and forms a trimeric complex with IL-1R3, and IL-1R6 binds IL-36 $\alpha$ , IL-36 $\beta$  and IL-36 $\gamma$ , similarly recruiting IL-1R3. In each case, IL-1R3 is the co-receptor that allows for dimerization of the cytoplasmic TIR domains, triggering a unique response<sup>8, 9</sup>. With IL-1R3 being the signaling regulator for six different cytokines, there are IL-1R3 dependent cytokines inducing inflammation, a T<sub>H</sub>1 response, a T<sub>H</sub>2 response or a combination of inflammation with either T<sub>H</sub>1 or T<sub>H</sub>2 responses. Blocking a common co-receptor rather than individual primary receptors or ligands, may therefore provide a new mode of action for reducing associated diseases.

We describe here for the first time a fully humanized blocking mAb targeting human IL-1R3 (MAB-hR3), with an incorporated Fc-LALA mutation to prevent triggering of Fc $\gamma$ Rs<sup>10, 11</sup>. We determined direct in vitro inhibition of signaling through IL-1R1, IL-1R4 and IL-1R6 by this mAb and investigated the inflammatory contribution of the IL-1R3 signaling associated cytokines. Additionally, we conducted proof-of-concept in vivo studies using a mouse IL-1R3 mAb (MAB-mR3) in models of IL-1 $\beta$ -dependent monosodium urate crystal (MSU) peritonitis, IL-33 dependent ovalbumin (OVA) allergic airway inflammation and IL-36 dependent imiquimod (IMQ)-induced psoriasis. In each case, IL-1R3 blockade proved effective in attenuating the disease phenotypes.

## Results

### MAB-hR3 binds dose-dependently, specifically and with high affinity to human IL-1R3.

We initially examined the binding properties of MAB-hR3. MAB-hR3 is a humanized IgG1 Fc-LALA mutated IL-1R3 mAb, produced in wild-type albino zika rabbits. We observed dose-dependent binding to an IL-1R3 expressing human melanoma cell line, SK-MEL-30 ( $EC_{50} = 274$  ng/mL,  $K_D = 1.73$  nM, assuming complete specific binding Fig. 1a).

Comparing MAB-hR3 to an IgG isotype control on both the human SK-MEL-30 cell line (Fig. 1b) and the murine cell line NIH-3T3 (Fig. 1c), we observed species specificity and ruled out non-specific binding (gating strategy Supplementary Fig. 1a).

Next, we demonstrated that MAB-hR3 binds human IL-1R3 using immunoprecipitation. MAB-hR3 was incubated with A549 cell lysates, immunoprecipitated and subjected to analysis by mass-spectrometry (MS). We confirmed the presence of IL-1R3 peptides in the MAB-hR3 immunoprecipitation (Supplementary Fig. 1b), whereas no IL-1R3 peptides were observed using an IgG isotype control (Data not shown). Since we did not observe non-specific binding of MAB-hR3 to any common sequence of IL-1 family receptors which share homologous IgG domains. The data observed when using MAB-hR3 could not be due to specific binding of multiple IL-1 family receptors simultaneously, but rather IL-1R3 specific effects. Formal binding kinetics for MAB-hR3 to human IL-1R3 were established using surface plasmon resonance (SPR) ( $K_D = 415$  pM) (Fig. 1d).

MAB-hR3 has an incorporated double substitution L234A/L235A (LALA) mutation, which significantly reduces binding to Fc $\gamma$ Rs<sup>10</sup>. This was confirmed in an antibody dependent cellular cytotoxicity (ADCC) bioassay, measuring NFAT activation in Fc $\gamma$ RIIIa expressing Jurkat effector cells as a readout of FcR triggering. Here, MAB-hR3 with- and without the incorporated mutation were compared (Fig. 1e). We observed that the LALA mutation completely abrogated Fc $\gamma$ R dependent activation of the NFAT reporter, indicating a lack of cytotoxic potential. In line with this, incubating MAB-hR3 (1  $\mu$ g/mL or 20  $\mu$ g/mL) with peripheral blood mononuclear cells (PBMCs) did not reveal any significant change in a WST-1 cell proliferation assay compared to control. Also, we did not observe an increase in IL-6 production as an indication of Fc-mediated agonistic properties (Supplementary Fig. 1c, d)<sup>12,13</sup>.

### **MAB-hR3 inhibits signaling for IL-1R1, IL-R4 and IL-R6.**

We evaluated the ability of MAB-hR3 to inhibit signaling through the three IL-1R3 associated ligand binding receptors; IL-1R1, IL-1R4 and IL-1R6. For each pathway, we used modified gene-reporter cell lines expressing the receptor of interest comparing with a polyclonal IL-1R3 blocking antibody. To determine IL-1R1 signaling interference using IL-1R3 blockade, we used IL-1 $\alpha$  stimulation of an A549 luciferase reporter cell line measuring NF- $\kappa$ B activation (IC<sub>50</sub>: MAB-hR3 = 146 ng/mL, Fig. 2a). For IL-1R4, we used IL-33 stimulation of a HEK293 SEAP reporter cell line (NF- $\kappa$ B/AP-1 activation, IC<sub>50</sub>: MAB-hR3 = 749 ng/mL, Fig. 2b). Lastly, IL-1R6 interference was investigated using IL-36 $\gamma$  stimulation of a HEK293/17 luciferase reporter cell line (NF- $\kappa$ B activation, IC<sub>50</sub>: MAB-hR3 = 17.1 ng/mL, Fig. 2c). Significant inhibition was observed in each of the three assays at low concentrations.

Next, we evaluated the inhibition of cytokine production from cells lines without reporter modifications. We used MAB-hR3 concentrations ranging from 1  $\mu$ g/mL (6.9 nM) to 20  $\mu$ g/mL (138 nM). We used native A549 cells for IL-1 $\alpha$  induced IL-6 production, a human mast cell line (HMC-1) for IL-33 induced IL-8 production and a human keratinocyte cell line (HaCaT) for IL-36 $\alpha$  induced IL-8 production.

In the A549, HMC-1 and HaCaT cell lines, MAB-hR3 decreased cytokine production significantly by up to 74% (IL-6), 28% (IL-8) and 57% (IL-8), respectively (Fig. 2d–f). MAB-hR3 showed a clear dose-dependent inhibitory response in both A549 and HMC-1 cells, however inhibited with similar efficacy at each concentration used in HaCaT cells. To verify the influence of IL-1 signaling in these cell lines, we also examined IL-1Ra (anakinra) as an inhibitor. We used a concentration of IL-1Ra (10 µg/mL (578 nM)), which is 10-fold greater than the maximum blood level in rheumatoid arthritis patients treated with a standard clinical dose of 100 mg subcutaneously. IL-1Ra had a statistically significant impact on IL-1α-induced IL-6 production in A549 cells (92% decrease), whereas no significant reductions were observed on IL-33 nor IL-36α induced IL-8 production. Underlining that the effect of MAB-hR3 in these cell lines were not related to IL-1R1 signaling inhibition.

### Binding of soluble IL-1R3 does not abrogate the anti-inflammatory effects of MAB-hR3

IL-1R3 is found in a soluble form (sIL-1R3) in the circulation where it increases the neutralization capacity of IL-1R2. IL-1β binds to the soluble decoy-receptor IL-1R2 (sIL-1R2). When sIL-1R3 binds to this complex, the affinity to bind IL-1β increases by ~100-fold<sup>14</sup>. Hence, sIL-1R3 functions as an anti-inflammatory receptor. In the circulation, there is an excess amount of sIL-1R3 (approx. 300 ng/mL in plasma) compared to sIL-1R2 (approx. 7 ng/mL in plasma)<sup>14</sup>, both beyond the circulating levels of IL-1β (mean level of 0.33 pg/mL in 500 healthy subjects<sup>15</sup>).

To determine whether MAB-hR3 would affect the anti-inflammatory function of sIL-1R3, we used whole-blood cultures to mimic the conditions of MAB-hR3 infusions in humans. We initially confirmed the presence of sIL-1R1, sIL-1R2, sIL-1R3 and sIL-1R4 (Fig. 2g). Using heat-killed *Candida albicans* to mimic an inflammatory condition via dectin-1 and TLR2 receptors<sup>16, 17</sup>, we measured IL-17 and IL-6 levels in the presence of MAB-hR3. Suppression of IL-17 and IL-6 production by MAB-hR3 takes place in whole-blood cultures containing sIL-1R3 (Fig. 2h, i). The importance of IL-1 in these cultures is illustrated by the ability of IL-1Ra to reduce IL-17 and IL-6 production by 77% and 96%, respectively. We conclude that any neutralization of endogenous sIL-1R3 by MAB-hR3 does not significantly impair the IL-1 blocking mechanism of soluble or cell bound IL-1R2 in a complex with sIL-1R3.

We further evaluated the impact of MAB-hR3 on IL-1 dependent IL-6 production. We pre-incubated a fixed concentration of MAB-hR3 with increasing concentrations of recombinant sIL-1R3, in order to “decoy” MAB-hR3 to bind to sIL-1R3. Increasing concentrations of sIL-1R3 did, in fact, reduce the inhibitory effect of MAB-hR3 as measured by IL-6 production (Fig. 2j). However, since there was no effect on *C. albicans*-induced IL-6 production in the presence of increasing concentrations of recombinant sIL-1R3 alone (Fig. 2k), the decreased effect of MAB-hR3 was due to freely available antibody and not an anti-inflammatory function of sIL-1R3 itself. We conclude that although MAB-hR3 can be “decoyed” to sIL-1R3, MAB-hR3 retains its ability to block IL-1R3 surface receptors and provide a robust reduction in inflammation.

## Blocking IL-1R3 reduce monosodium urate (MSU) crystal mediated peritonitis

In order to study the effects of blocking IL-1R3 in models of human disease, we developed chimeric mouse IgG2a Fc-LALA mutated IL-1R3 mAb (MAB-mR3), using wild-type albino zika rabbits for immunization. We used SPR to confirm the development of a high-affinity antibody ( $K_D = 63\text{pM}$ ), as well as functional testing and comparison to MAB-hR3 (Supplementary Fig. 2).

We sought to address the differences of IL-1R3 blockade compared to IL-1R1 blockade. The clinically established treatments of the IL-1R1 signaling pathway, and the importance of IL-1 in the development of co-morbidities justified this comparison. Thus, we administered the antibody to mice challenged with MSU crystal induced peritonitis, a model highly dependent on IL-1 $\beta$ <sup>18</sup>. Notably, this model also possesses some of the multifaceted interactions that take place in an acute gout attack, including morphological similarities between the synovium and peritoneal lining<sup>19</sup>. Animal models using MSU as well as humans with recurrent gout attacks respond dramatically to IL-1 $\beta$  blocking therapies<sup>18, 19, 20</sup>.

In MSU-induced peritonitis, the inflammation is due to white blood cell (WBC) influx to the peritoneal cavity. We observed a marked decrease in the total number of WBC in the MAB-mR3 treated group compared to the vehicle-treated group (Fig. 3a). The decrease was consistent across multiple cell types; granulocytes (65% decrease), monocytes (57% decrease) and lymphocytes (42% decrease) (Fig. 3c). In the IL-1Ra treated group, we observed a similar pattern, although less pronounced compared to that observed in the MAB-mR3 treated mice. In addition, protein concentration in the intraperitoneal (IP) fluid was evaluated as a marker of plasma protein leak, corresponding to the intensity of inflammation. Here, we observed no significant changes in any of the treatment groups (Fig. 3b).

We compared the levels of IL-1 $\beta$  in the peritoneal WBC lysates from MSU treated mice. In the MAB-mR3 treated group, the mean IL-1 $\beta$  concentration level was 69% lower than in vehicle treated mice (Fig. 3d). Total IL-1 $\beta$  in cell lysates consists of both IL-1 $\beta$  precursor and matured IL-1 $\beta$ . This indicates that the amount of both mature IL-1 $\beta$  and its precursor available for caspase-1 mediated release is significantly decreased in the MAB-mR3 group, but not in the IL-1Ra treated mice. To evaluate whether this was solely related to cell frequencies, we calculated the levels of IL-1 $\beta$  per million WBC. Here, we still observed significantly lower levels of IL-1 $\beta$  (34%) in the MAB-mR3 treated mice compared to the vehicle control group (Fig. 3e). In contrast, we did not observe a decrease of IL-1 $\beta$  per cell in the IL-1Ra treated group. We observed a significant difference in intracellular IL-1 $\beta$  levels between MSU recruited WBC from MAB-mR3 compared to IL-1Ra treated mice (53% difference, Fig. 3d), which was also observed when normalized to WBC (47% difference, Fig. 3e). Together, these data show that IL-1R3 blockade is more effective in reducing inflammation compared to IL-1R1 blockade in the MSU-induced peritonitis model.

Neutrophils are important effectors in innate immunity, actively recruited in the early phases of an inflammatory response. Thus, the observed decrease in granulocyte influx could also reflect some of the challenges that can be faced when inhibiting innate cytokines. In gout,

neutrophils are however the most abundant cells, degranulating as the cell phagocytizes the urate crystals. Here, the granule enzymes intensify inflammation and are damaging to tissues<sup>21, 22</sup>. In line with this, we observed a significant increase in the concentration of elastase in the IP fluid from MSU injected mice compared to saline injected mice. In the mice exposed to MSU, MAB-mR3 significantly decreased IP fluid elastase by 48% (Fig. 3f). Further, elastase concentrations in IP cell lysates from MSU injected mice decreased by 72% in the MAB-mR3 group, and by 50% in the IL-1Ra group (Fig. 3g). IP cell lysate myeloperoxidase (MPO) levels decreased by 68% in MAB-mR3 treated and by 51% in the IL-1Ra treated group compared to vehicle controls (Fig. 3h).

Granulocyte colony stimulating factor (G-CSF), a neutrophil attractant and activator, and IL-6 are induced by MSU. Both were however reduced in the IP fluid from mice treated with MAB-mR3, whereas IL-1Ra did not significantly impact IL-6 levels (Table 1). Similar data was observed for the chemokines CXCL-1 (KC), CCL-2 (MCP-1) and CCL-3 (MIP-1 $\alpha$ ). All increased by MSU, and were reduced following MAB-mR3 treatment, where CXCL-1 and CCL-2 reached statistical significance (Table 1). The IL-1Ra treated group did not exhibit a decrease in any of the chemokines assessed. Also, circulating IL-6 and G-CSF elevated by MSU, were significantly decreased by both MAB-mR3 and IL-1Ra (Table 1). CXCL-1 in lysed whole blood seemed to decrease in the MAB-mR3 group but was unaffected in the IL-1Ra treated group. Both MPO and CXCL-1 were significantly lowered in spleen lysates using MAB-mR3, whereas IL-1Ra again was less effective and showed no impact on CXCL-1 (Table 1). Collectively, these data indicate a broader impact of IL-1R3 blockade compared to blocking IL-1R1 alone.

### **IL-1R3 blockade broadly inhibits cytokine production compared to single pathway inhibition**

Having shown the efficacy of IL-1R3 blockade compared to IL-1R1 blockade in the MSU model, we next examined the differential impact of blocking either IL-1R3 (using MAB-hR3), IL-1R4 (using sIL-1R4 (sST2)) or IL-1R6 (using IL-36Ra). We used heat-killed *C. albicans* stimulations of freshly isolated PBMCs to address IL-6 and IFN- $\gamma$  production. We found that blocking IL-1R3, but not signaling of IL-33 (through IL-1R4) or IL-36 (through IL-1R6), decreased the production of IL-6 by 67% (Fig. 4a). In contrast, the production of IFN- $\gamma$  was significantly inhibited by blocking each of the three receptors (Fig. 4b). Thus, blocking IL-1R3 compared to the inhibition of IL-33 or IL-36 signaling, revealed a wider impact of targeting IL-1R3. Yet, these data also revealed a clear importance of IL-33 and IL-36 signaling in the *C. albicans* induced production of IFN- $\gamma$ . Still, this dependency is not observed in the production of IL-6 where solely IL-1R3 signaling is contributing.

We next used a two-way Mixed Leukocyte Reaction (MLR) as an endogenous inducer of cytokines. During a 5-day co-culture of PBMCs from two unrelated healthy donors, multiple cytokines are produced allowing us to dissect any differences between IL-1R1 and IL-1R3 signaling more broadly. We found that MAB-hR3 significantly decreased the production of IFN- $\gamma$ , IL-13, IL-17, IL-22, TNF, IL-6 and IL-10 (Fig. 4c-i). In contrast, inhibition of IL-1 $\alpha$  and IL-1 $\beta$  signaling by IL-1Ra impacted only four cytokines: IFN- $\gamma$ , IL-17, IL-22 and IL-10

(Fig. 4c, e, f, i). Thus, blocking IL-1R3 provides broader anti-inflammatory effects, compared to IL-1R1 blockade (IL-1Ra).

### **Anti-IL-1R3 ameliorates ovalbumin (OVA)-induced inflammation in vivo**

The wide anti-inflammatory effects of IL-1R3 blockade suggested investigations into other models of human disease. Thus, we examined the OVA-induced allergic airway inflammation model, known for its IL-33 dependency<sup>23</sup>. Mice were fully sensitized with OVA before being treated with MAB-mR3. As expected, the challenge of intratracheal OVA resulted in high numbers of WBC in the lungs, as measured in the bronchoalveolar lavage (BAL) fluid (Fig. 5a). Here, MAB-mR3 treatment resulted in a 46% decrease in the number of WBC infiltrating the lungs and a similar (46%) decrease in eosinophils (Fig. 5b). Likewise, we observed a decrease in the content of both alveolar macrophages and neutrophils, the latter being highly significant.

We repeated the model to include measures of BAL fluid cytokines, mucus production and airway responsiveness, using the same sensitization schedule, but with aerosolized OVA as the challenge. We observed a similar significant decrease in the influx of WBC in the BAL fluid (50%) as in the first experiment. Further, we observed a significant 54% decrease of the BAL cytokine IL-4, whereas IL-5, IL-13, IL-6 and TNF all decreased (63%, 64%, 76% and 33%, respectively), but not significantly (Fig. 5c). Histology examination of the lungs confirmed the difference between OVA alone and blocking inflammation using MAB-mR3. The difference was evident on both infiltrating immune cells (H&E), and the significant decrease in mucus producing goblet cells in the airways (PAS) (Fig. 5d+e). Changes in airway responsiveness were assessed using a methacholine (MCh) provocation test. We found that MAB-mR3 significantly decreased airway resistance at both 25 mg/mL, 50 mg/mL and 100mg/mL of MCh, respectively (Fig. 5f), and observed no significant differences between MAB-mR3 treated and vehicle mice at any dose of MCh. Thus, MAB-mR3 limits both inflammation and related functional measures in this disease model.

### **Anti-IL-1R3 ameliorates imiquimod (IMQ)-induced psoriasis attenuated in vivo**

Mutations in IL-36Ra are linked to human pustular psoriasis<sup>24, 25</sup>. Blocking the IL-36 signaling pathway through IL-1R3 could therefore alleviate this disease. We investigated MAB-mR3 in the IMQ-induced psoriasis mouse model<sup>26</sup>. We observed that the MAB-mR3 treated mice showed less weight loss compared to vehicle treated IMQ-challenged mice (day 4) (Fig. 6a). Secondly, an unblinded erythema score revealed a significant difference on the last day of the experiment between MAB-mR3 and IMQ-mice (Fig. 6b). This anti-inflammatory effect was also observed in the ear thickness of mice receiving IMQ or vehicle cream on one ear, and control cream on the other. Here, we observed a striking difference between groups, with significantly less ear swelling (IMQ/control) in the MAB-mR3 treated group (day 6) (Fig. 6c).

Next, skin inflammation for each mouse was scored by 6 individuals, each blinded to the treatment. The score was based on erythema, thickness and skin scaling (collective scale from 0–4, modified PASI). The MAB-mR3 treated group was graded with significantly lower scores than mice not receiving treatment (Fig. 6d, examples of scoring depicted). We

similarly found the numbers of circulating granulocytes on the day of sacrifice were significantly less (32% decrease) in MAB-mR3 treated mice ( $p=0.03$ ) (Fig. 6e). But also the concentration of MPO in the skin was lower (69%) (Fig. 6f), indicative of lower numbers of neutrophils in the skin, less neutrophil degranulation or both. A clear correlation between the visual scores and the levels of MPO underlined the importance of these observations (Fig. 6g).

Lastly, we measured the transcriptional changes in the skin. We observed that topical application of IMQ significantly upregulated IL-36 $\alpha$  mRNA levels in the skin, but not IL-36 $\beta$  or IL-36 $\gamma$ . MAB-mR3 treatment did not affect expression for either of the IL-36 subtypes (Fig. 6h–j). We also determined mRNA levels of IL-17a, IL-17f and IL-22, known key-regulators in the pathogenesis of psoriasis. Here, we observed that blocking IL-1R3 using MAB-mR3 significantly decreased the transcription of all three cytokines; IL-17a (66%), IL-17f (83%) and IL-22 (96%). Thus, a single therapeutic intervention can markedly reduce multiple important mediators of disease, disclaiming the need for multiple cytokine interventions.

## Discussion

Dysregulation of the innate immune system takes place in atherosclerosis, autoimmune diseases, Alzheimer's disease and cancer<sup>27, 28, 29, 30</sup>. For example, a global trial of 10,000 patients at risk for a second heart attack or stroke revealed that specific neutralization of IL-1 $\beta$  reduced both atherosclerosis and heart failure, but also the incidence- and survival of cancer<sup>31, 32</sup>. Thus, innate inflammation can be reduced by lowering the level of IL-1 $\beta$ . Accordingly, our hypothesis is that blocking IL-1R3 can reduce both the specific cytokine of a disease, for example IL-33 in asthma, as well as the associated dysregulated IL-1 component driving basal inflammation contributing not only to the disease phenotype, but also to the development of co-morbidities.

In the present study, we addressed responses specific for IL-1, IL-33 and the IL-36 subfamily, and found that blocking IL-1R3 is highly effective in models of peritonitis, allergic airway inflammation and psoriasis. In each of these models, there is an inflammatory component from either IL-1 $\beta$  or IL-1 $\alpha$ . In the case of MSU peritonitis, IL-1 $\beta$  is the primary disease driving cytokine. In asthma or psoriasis, inflammation from IL-1 worsened the severity of the disease manifestation.

The initial *in vitro* data supported the rationale for examining the broad effects of IL-1R3 blockade *in vivo*. Since MSU induced inflammation is primarily driven by IL-1 $\beta$ , IL-1Ra was used as the positive control for efficient IL-1R1 inhibition. Despite using a 4-fold higher molar dose of IL-1Ra compared to MAB-mR3, blocking IL-1R3 provided a surprisingly additional level of protection. We speculate that blockade of the alarmin effects of IL-33 in barrier cells<sup>33</sup>, such as the peritoneal lining, might be of importance. IL-33 is traditionally known to induce a T<sub>H</sub>2 dominated inflammation. However, in both the peritoneal cavity and in the skin, IL-33 induces a predominant neutrophil milieu as observed here<sup>34, 35</sup>.

Caspase-1 inhibition can similar be effective in MSU models<sup>20</sup>. However, extracellular cleavage of the IL-1 $\beta$  precursor by neutrophilic elastase and proteinase 3 can similar result in generation of active mature IL-1 $\beta$ <sup>36,37</sup>. Thus blocking IL-1 receptors is likely superior in diseases such as neutrophil-predominant arthritis, where elastase contributes substantially to IL-1 $\beta$  driven inflammation<sup>37</sup>. In our MSU model, we observed a significant decrease in both granulocyte influx as well as elastase production when blocking IL-1R3 using MAB-mR3.

We next compared the effects of IL-1R3 blockade with that of specific IL-1R4 or IL-1R6 blockade. Here, we observed that T<sub>H</sub>1 responses driven by IL-33 or IL-36 cytokines can be reduced by IL-1R3 blockade. Secondly, that blocking IL-1R3 had a broader anti-inflammatory effect compared to isolated IL-33 or IL-36 signaling inhibition. Findings that were recapitulated when investigating the differences between IL-1R1 and IL-1R3 blockade using two-way MLRs. For that reason, we found cause to exploit IL-1R3 blockade in diseases influenced by multiple IL-1 family members. For instance the highly IL-33 dependent OVA-induced allergic asthma model<sup>38</sup>, as well as in the IL-36 dependent IMQ-induced psoriasis model<sup>39</sup>.

In the airways, IL-33 promotes a T<sub>H</sub>2 response, attracting eosinophils and basophils. MAB-mR3 treatment significantly reduced cell influx into the airways, primarily due to a marked decrease in eosinophils, important in allergen triggered airway inflammation<sup>40</sup>. We also observed a decrease in the levels of neutrophils, similar to the decrease observed in the MSU model. It is likely that the decrease in CXCL-1 (equivalent to human IL-8) could account for the lower numbers of neutrophils, as it is consistent with the known IL-8 induction in human airway goblet cells by IL-33<sup>41</sup>. Thus, decreasing airway inflammation by inhibition of both IL-1 and IL-33 induced IL-8 production, could be more effective than IL-33 blockade alone in allergic asthma, supporting IL-1R3 blockade. Consistent with these observations was a significant improvement of airway resistance to MCh challenge, revealing clear functional consequences of the anti-inflammatory intervention.

The IMQ model is similar dependent not only on IL-36, but also on IL-1 and IL-8, making this disease similar attractive for IL-1R3 blockade<sup>24,42,43</sup>. In our study, MAB-mR3 significantly attenuated visual signs of the disease, i.e. disease severity. And like the previously observed reduction of neutrophils by MAB-mR3, we also observed significantly lower numbers of circulating neutrophils as well as decreased levels of the neutrophil activation marker MPO in the skin. In fact, visual scoring correlated to levels of skin MPO. Remarkably there was a highly significant reduction of both IL-17a, IL-17f and IL-22 expression. These cytokines each possess an important role in the pathogenesis of psoriasis<sup>44</sup>, particularly for IL-22 where human mast cells produce large amounts of IL-22<sup>45</sup>. The observation that IL-1R3 blockade can inhibit the transcription of these cytokines supports a role for IL-1R3 targeting in psoriasis.

Although IL-1R3 is the co-receptor for ligand binding receptors of six different cytokines, IL-1R3 is not the only co-receptor shared by multiple cytokines. In fact, both the common  $\gamma$  chain (IL-2R $\gamma$ ) and glycoprotein 130 (gp130 or IL-6ST (signal transducer)) are likewise required for the signaling of multiple cytokines. However, mice deficient of IL-2R $\gamma$  or gp130 have developmental abnormalities such as leukocyte production (IL-2R $\gamma$ ) and organ

development(gp130), respectively<sup>46, 47</sup>. In contrast, IL-1R3 deficient mice display no signs of anatomic abnormalities and remain fully fertile<sup>48</sup>. Still, suppressing multiple signaling pathways could reduce the potential to mount an innate immune response, increasing frequencies of infections and impacting the development of T helper cells, such as T<sub>H</sub>1, T<sub>H</sub>2 and T<sub>H</sub>17. However, compared to using monotherapy such as anti-IL-33, using a lower dose of anti-IL-1R3 could still allow for a basic level of signaling through the primary pathways and remain disease suppressive. Considering the synergism between cytokines of the IL-1 family, reducing signaling in this family by IL-1R3 blockade, could likely easier revert a vicious cycle, than intervening in multiple unrelated pathways. Thus, future research needs to address these concerns and considerations.

In summary, blocking IL-1R3 is a novel therapy to limit activities from 6 members of the IL-1 family. With a broad applicability and specific targeting, this offers a feasible treatment option with an extensive therapeutic range.

## Methods section:

### Monoclonal antibody production and test of affinity.

Human recombinant protein was used as the immunogen for wild-type albino Zika rabbit immunization. Where after the isolated and modified humanized IgG1 monoclonal Fc-LALA mutated IL-1R3 antibody (MAB-hR3) were produced in HEK-293-FreeStyle cells (ThermoFisher Scientific). The antibody was purified from the supernatant using protein-A affinity chromatography followed by size exclusion chromatography (MAB Discovery GmbH). The mouse monoclonal chimeric IgG2a Fc-LALA mutated IL-1R3 antibody (MAB-mR3) was similar produced (MAB Discovery GmbH). However, using a specific mouse recombinant protein in an independent immunization campaign.

For both antibodies, binding characteristics were determined using SPR (Biacore T200) carried out by an external provider (Biaffin GmbH & Co KG). Single-cycle setups were done using increasing concentrations of human (0.111–9 nM) – or mouse (0.185–15 nM) IL-1R3, measuring the interaction with captured MAB-hR3 or MAB-mR3 respectively. Two independent measurements were performed for each tested antibody.

### Functional testing of MAB-hR3

Cell binding analyses of MAB-hR3 were carried out using NIH-3T3 (DMEM, 10% FCS) (ATCC) and SK-MEL-30 (RPMI, 10% FCS) (kindly provided by Prof. Mayumi Fujita) cell lines. Cells were harvested using Accumax (Sigma), washed and resuspended in stain buffer (BD Pharmingen), before incubating with MAB-hR3 (10 µg/mL) or human IgG isotype control (MAB Discovery) for 30min (4°C). For EC50 and affinity calculation of SK-MEL-30 cell binding, cells were incubated in a 1:2 dilution series with MAB-hR3 starting at 20 µg/mL. Cells were subsequently washed with stain buffer and incubated with Alexa-488 labelled goat-anti-human secondary antibody (Dianova) for 30min (4°C). Afterwards, the cells were washed with staining buffer and resuspended in buffer containing 1:100 diluted DRAQ7 (Abcam) dead cell stain. Samples were run on an Accuri C6 Sampler and analyzed using FlowJo (ThreeStar, New Jersey, USA).

Immunoprecipitation was done according to protocol using Dynabeads (Co-Immunoprecipitation kit, Life Technologies) coupled to MAB-hR3 (30 mg antibody/mg beads) or human IgG isotype control (30 mg antibody/mg beads, R&D Systems). A549 cells (ATCC) were stimulated in T175 flasks with recombinant human IL-1 $\alpha$  (5 ng/mL, 15min, Peprotech) to allow the cytokine associated signaling complex to form (IL-1R1+IL-1 $\alpha$ +IL-1R3). Cells were then lysed (1x IP buffer from kit, 100 mM NaCl and protease inhibitor (1X, Halt protease inhibitor cocktail, ThermoFisher scientific)) and the lysate divided equally and incubated (30min, 4°C) with either MAB-hR3 or IgG coupled beads (7.5 mg), followed by three washing steps.

The bound protein from the beads were eluted in buffer (0.5M NH<sub>4</sub>OH (14.8 N) and 0.5mM EDTA) and lyophilized in a centrifugal vacuum concentrator for 6 hours. Lyophilized proteins were solubilized in sample buffer (40% glycerol, 0.3M Tris, 0.3M SDS, 0.2M DTT and 0.6mM bromophenol blue in H<sub>2</sub>O) and heated at 37°C (30min) to avoid membrane protein aggregation. The samples were run on a 7.5% Mini-Protean TGX gel (BioRad).

The gels were stained with colloidal Coomassie<sup>49</sup> and visible bands including in-between areas were excised and sent to University of Colorado School of Medicine Biological Mass Spectrometry Facility for analysis. Here, gel pieces were destained (200  $\mu$ L of 25 mM ammonium bicarbonate in 50 % (v/v) acetonitrile, 15 min) and washed twice (200  $\mu$ L of 50% (v/v) acetonitrile). The disulfide bonds in proteins were reduced by incubation in 10 mM dithiothreitol (DTT) at 60 °C for 30 min and cysteine residues were alkylated with 20 mM iodoacetamide (IAA) in dark (room temperature, 45 min). Gel pieces were subsequently washed with 100  $\mu$ L of distilled water, followed by addition of 100  $\mu$ L of acetonitrile and dried on SpeedVac (Savant ThermoFisher). Next, trypsin (100ng) was added to each sample and allowed to rehydrate the gel plugs at 4 °C for 45 min after which they were incubated at 37 °C overnight. The tryptic mixtures were acidified with formic acid up to a final concentration of 1%.

Peptides were extracted two times from the gel plugs using 1% formic acid in 50% acetonitrile. The collected extractions were pooled with the initial digestion supernatant and dried on SpeedVac (Savant ThermoFisher). Samples were then analyzed on an LTQ Orbitrap Velos mass spectrometer (Thermo Fisher Scientific). This was coupled to an Eksigent nanoLC-2D system through a nanoelectrospray LC – MS interface as previously described<sup>50</sup>. We received a final report for the samples analyzed.

### **MAB-hR3 LALA mutation, PBMC viability and spontaneous cytokine production.**

To test the activity of IgG-1 and IgG1-LALA versions of the humanized anti-IL1R3 antibody in eliciting Fc-mediated effector cell functions such as ADCC, MAB-hR3 was tested both with- and without an incorporated LALA mutation. We used a bioassay, measuring the antibody induced activity of a gene-reporter (NFAT) in Fc $\gamma$ RIIIa expressing Jurkat effector cells, thus not a classical ADCC assay. Briefly, hIL-1R3 expressing target cells SK-MEL-30 cells were seeded in a 384-well tissue-culture treated plate at a density of 2500 cells/well in 25 $\mu$ l RPMI medium containing 10% FCS. 24h after seeding, 4000 effector cells/well (ADCC Bioassay Effector cells, Jurkat, Promega) were added in RPMI medium containing 4% low-IgG-FCS. Antibodies were then added to a final concentration ranging

from 0.002 ng/mL to 10000 ng/ml, and the plate was incubated for 6 hours at 37°C and 5 % CO<sub>2</sub>. Activation of NFAT signaling in luciferase gene reporter Jurkat cells was measured according to manufacturer's instructions (Bio-Glo Luciferase Assay) using a Tecan M1000 microplate reader.

Next, we evaluated the impact of MAB-hR3 on PBMCs using a conventional MTT reduction assay (Roche). PBMCs (500,000/well) from three healthy donors were incubated with either medium or MAB-hR3 (1µg/mL or 20µg/mL). For the 24 hours experiments, we used 96-well flat bottom plates without FCS in the medium, and for the 3 and 5 days, round bottom wells with 10% FCS in the medium. The cells were assayed in triplicates after either 24hrs, 3 or 5 days. On the day of analysis, PBMCs were incubated 2 hours with MTT (20µL in 200µL) before adding MTT solvent for 15min and measuring absorbance at 570 nm on an ELISA reader. Using the linearity between absorbance and viable cells converting MTT, we calculated the number of viable cells using medium alone as the control set to 100%. At same day of MTT analysis, we also harvested supernatants from PBMCs incubated under same conditions and from same donors, subsequently assaying for IL-6 production.

### Cell line experiments.

An A549 (NF-κB) Luciferase reporter cell line (Signosis, DMEM, 10% FCS) (37°C/5% CO<sub>2</sub>) was used for IL-1R1 investigation. Cells were seeded in 384-well flat bottom plates (40,000 cells/well), rested for 16hrs before pre-incubating 1hr with MAB-hR3 or polyclonal (goat-anti-human-IL-1R3, R&D Systems) antibody at increasing concentrations. Recombinant human IL-1α (0.1ng/mL, R&D Systems) was added for 5hrs. Steady-Glo™ (Promega) solution was used on lysates for development and luminescence measured using a Tecan M1000 plate reader. The A549 cell line (ATCC) was cultured in T75 flasks (37°C/5% CO<sub>2</sub>) in complete F-12K media (10% FCS). Cells were seeded in 96-well flat bottom plates (50,000/well) and rested for 3hrs before pre-incubating 1hr with MAB-hR3 (1 – 20µg/mL) or IL-1Ra (10µg/mL). Cells were stimulated with recombinant human IL-1α (50pg/mL, Peprotech) for 24hrs and assayed for IL-6 production.

Inhibition of signaling through IL-1R4 was investigated using HEK-Blue™ SEAP reporter IL-33 cell line (NF-κB/ AP-1 activation) (InvivoGen) (DMEM, 10% FCS) (37°C/5% CO<sub>2</sub>). Cells were seeded in 384-well flat bottom plates (25,000 cells/well), rested 16hrs before pre-incubating 1hr with MAB-hR3 or polyclonal (goat-anti-human-IL-1R3, R&D Systems) antibody at increasing concentrations. Recombinant human IL-33 (5ng/mL, R&D Systems) was added and plates incubated overnight. Supernatants were transferred to clear, flat bottom polystyrene NBS™ microplates (Corning) containing 2xQUANTI-Blue reagent (InvivoGen) and incubated (37°C for 45min) before measuring optical density (655nm) using a Tecan M1000 plate reader. The human mast cell line (HMC-1) (Kindly provided by Prof. SooHyun Kim) was used to investigate the impact on IL-33 induced IL-8 production. The cell line was cultured in T75 flasks (37°C/5% CO<sub>2</sub>) in complete Iscovés modified Dulbeccó's medium (IMDM, 10% FCS, 1% Pen/Strep.). HMC-1 cells were seeded in 96-well flat bottom plates (50,000/well) and rested for 3hrs before pre-incubating 1hr with MAB-hR3 (1 – 20µg/mL) or IL-1Ra (10µg/mL). Cells were stimulated with recombinant human IL-33 (20ng/mL, R&D Systems) for 24hrs and assayed for IL-8 production.

Inhibition of signaling through IL-1R6 were investigated using a HEK293/17 luciferase reporter cell line (NF- $\kappa$ B activation) (MAB Discovery GmbH) (DMEM, 10 % FCS, 20 $\mu$ g/ml hygromycin) (37°C/5% CO<sub>2</sub>). Cells were seeded out in 384-well flat bottom plates (30,000/well) and rested for 16hrs before pre-incubating 1hr with MAB-hR3 or polyclonal (goat-anti-human-IL-1R3, R&D Systems) antibody at increasing concentrations. Recombinant human IL-36 $\gamma$  (15ng/mL, R&D Systems) was added and incubated for 5hrs. Steady-Glo™ (Promega) solution was used on lysates for development and luminescence measured using a Tecan M1000 plate reader. The impact on IL-36 induced IL-8 production was investigated using a human keratinocytic cell line (HaCaT) (Kindly provided by Prof. Mayumi Fujita). The cell line was cultured in T75 flasks (37°C/5% CO<sub>2</sub>) in complete DMEM (10% FCS). HaCaT cells were seeded in 96-well flat bottom plates (50,000/well) and rested for 3hrs before pre-incubating 1hr with MAB-hR3 (1– 20 $\mu$ g/mL) or IL-1Ra (10 $\mu$ g/mL). Cells were stimulated with recombinant human IL-36 $\alpha$  (50ng/mL, R&D Systems) for 24hrs and assayed for IL-8 production.

### **Cytokine production in whole-blood reactions with soluble IL-1R3.**

Using freshly obtained blood (Heparin tubes), 250 $\mu$ L was pre-incubated with 550 $\mu$ L RPMI (No FCS) and 100 $\mu$ L of inhibitor (media, MAB-hR3 or IL-1Ra). After 1hr, 100 $\mu$ L of stimulant was added using medium or heat-killed *C. albicans* (0.5 $\times$ 10<sup>6</sup>/mL)<sup>51</sup>. After 24hrs of incubation, supernatants were harvested and analyzed for sIL-1R1, sIL-1R2, sIL-1R3, sIL-1R4, IL-6 or IL-17 production. For sIL-1R3 investigation, we used recombinant human IL-1R3 protein (R&D Systems). To test for binding to MAB-hR3, we pre-incubated (14hrs) MAB-hR3 (1 $\mu$ g/mL) with sIL-1R3 (62.5–1000ng/mL) before adding 100 $\mu$ L of this mix to the h.k. *C. albicans* stimulations as the inhibitor. To investigate the anti-inflammatory effect of sIL-1R3 alone, we used increasing concentrations (62.5–1000ng/mL) of sIL-1R3 without MAB-hR3 as inhibitor in the setup.

### **Functional testing of anti-mouse IL-1R3 (MAB-mR3) and comparison to MAB-hR3.**

The functionality of MAB-mR3 was tested in murine NIH-3T3 (NF- $\kappa$ B) Luciferase reporter cell lines (Signosis, DMEM, 10% FCS). Seeded in 384-well flat bottom plates (20,000 cells/well (30,000 cells/well for IL-33 stimulations)) and rested for 16hrs (37°C/5% CO<sub>2</sub>) before pre-incubating 1hr with MAB-mR3 antibody at increasing concentrations. Recombinant mIL-1 $\beta$  (50pg/mL), mIL-33 (1ng/mL) or mIL-36 $\gamma$  (170ng/mL) (R&D Systems) was added and plates incubated for 5hrs (37°C/5% CO<sub>2</sub>). Steady-Glo™ (Promega) solution was used on lysates and luminescence measured (Tecan M1000 plate reader). Inhibition of IL-6 release was determined in a NIH-3T3 cell line (ATCC). Seeded in 384-well flat bottom plates (12,500 cells/well) and rested for 2hrs (37°C/5% CO<sub>2</sub>) before pre-incubating 1hr with MAB-mR3 or MAB-hR3 antibody at increasing concentrations. Cells were stimulated with recombinant hIL-1 $\beta$  (50pg/mL, R&D Systems) for 16hrs and assayed for IL-6 production.

### **Monosodium urate crystal (MSU) peritonitis model.**

MAB-mR3 was administered to wild-type 8weeks old C57BL/6J male mice (Jackson Laboratories). Monosodium urate crystal (MSU)-induced peritonitis was induced with 3mg of MSU (diluted in 200 $\mu$ L PBS, Invivogen) per mouse by intraperitoneal (IP) injection. MAB-mR3 (500 $\mu$ g/mouse (17.2 $\mu$ M), MAB Discovery) was compared to IL-1Ra (anakinra,

10mg/kg (232µg/mouse (67.1µM.)) as the inhibitor (200µL/mouse). The four groups were comprised of: saline as vehicle control for MSU and inhibitor ( $n=4$ ), MSU alone with saline as inhibitor ( $n=8$ ), MSU with MAB-mR3 ( $n=8$ ) and the last group with MSU and IL-1Ra ( $n=8$ ). Each intervention group was represented by at least one mouse in each cage. MAB-mR3, IL-1Ra or saline was injected IP 1hr before MSU stimulation. The mice were euthanized 6 hours after MSU or saline injection. Blood was collected in micro-centrifuge tubes containing EDTA and peritoneal fluid collected by lavage using 10mL of ice-cold PBS. Organs were immediately frozen in liquid nitrogen. Plasma and whole-blood lysate (TritonX 0.5%) were assayed for cytokines. The differential number of cells collected by centrifugation (300g, 10min) of IP fluid was counted (HESKA HemaTrue) and lysed (TritonX 0.5%). Cytokines were measured in both IP fluid and IP cell lysates. For low abundance cytokines in the IP fluid, 8mL of fluid was concentrated (end range: 4.7– 10.9x concentrated) in pre-boiled (15min) dialysis membranes (MWCO 3.5kDa., Spectra/Por3 Dialysis membrane, Spectrumlabs) submerged in polyethylene glycol (MN 6–8000, Sigma Aldrich) as the hygroscopic solution (4°C). Initial concentrations were calculated by dividing with the dialysis concentration factor. Spleen lysates were assayed for cytokine levels and normalized to protein concentration of the lysates. Protein levels in spleen lysates and IP fluid were assayed with a standard Bradford assay, using protein assay dye reagent (BioRad) and BSA as a standard.

#### **PBMC stimulations and mixed leukocyte reactions.**

For PBMC stimulations, we used 500,000 freshly isolated PBMCs/well in 96-well round bottom plates, total volume of 200µL. Cells were seeded and incubated with either medium alone, MAB-hR3 (69nM (10µg/mL)), sIL-1R4 ((69nM (4.3µg/mL)) (R&D Systems), IL-36Ra (69nM (1.2µg/mL)) (R&D Systems) or IL-1Ra (587nM (10µg/mL)) for 1hr before stimulation. PBMCs were then stimulated with heat-killed *C. albicans* ( $0.5 \times 10^6$  microorganisms/mL, 5days, RPMI 10%FCS). After stimulation, supernatants were harvested and assayed for cytokine production.

In two-way mixed leukocyte reactions (MLR), we combined freshly isolated PBMCs from two unrelated healthy donors. PBMCs were mixed in a 1:1 ratio in 96-well round bottom plates (250,000 cells /donor, 200µL final volume) and incubated for 5days (RPMI, 10%FCS) with either medium alone, MAB-hR3 (5– 20µg/mL) or IL-1Ra (10µg/mL). Cytokine production was measured in the supernatants using both the Quansys multiplex platform and ELISA (Duoset, R&D Systems).

#### **Ovalbumin (OVA) allergic airway inflammation model.**

For the first OVA experiment (Exp.1), we used wild-type 6weeks old C57BL/6J male mice (Jackson Laboratories), sensitized IP using OVA (15µg/ 100µL, Sigma-Aldrich) mixed 1:1 with Imject Alum Adjuvant (100µL, ThermoFischer). In the second experiment (Exp. 2), we similar used wild-type 6weeks old C57BL/6J male mice (Jackson Laboratories) but sensitized using a lower concentration of OVA (10µg/ 100µL, Sigma-Aldrich) mixed 1:1 with Imject Alum Adjuvant (100µL, ThermoFischer). For both exp. 1+2, mice were injected at day 1, 14 and 21. At day 25–28 mice were injected IP with MAB-mR3 (500µg/mouse, MAB Discovery) or mouse IgG control (500µg/mouse, MAB Discovery).

For Exp.1, intratracheal instillation of OVA (50µg/mouse in 50µL) was done 30min post-injection at day 26–28 in short-term carbon dioxide anesthesia. Exp. 2 used aerosolized OVA (1% w/v in PBS). BAL was carried out as previously described by inserting a catheter into the trachea and washing the airways with  $3 \times 1\text{mL}$  washes<sup>52</sup>. BAL cells were enumerated by trypan blue exclusion. This was followed by cell phenotyping using flow cytometry (Exp.1.) or cytopinned and stained with Diff-Quick (DADE diagnostics, Germany) (Exp. 2). The following monoclonal antibodies (mAbs) against mouse targets were used for flow cytometry following mouse Fc Block (BD Biosciences): PE-Cy7 CD11c (N418), PerCP-Cy5.5 CD11b (M1/70), FITC-Ly6G (1A8-Ly6G) (all eBioscience); PE-Siglec-F (E250–4440) (from BD Biosciences) (1:400 dilution for all mAbs) (stained in DPBS containing 10mg/ml BSA, 0.1mg/ml NaN<sub>3</sub>) (Gating strategy in supplementary Figure 3). Cells were analyzed on a Canto II flow cytometer using FlowJo software (Treestar). Following BAL, the lungs were standard inflated with 4% PFA for 20 minutes with a pressure of 20 cm water column and subsequently stored in formalin overnight. Afterwards, lungs were embedded in agarose and cut in 2 mm thick slices according to the orientator principle. Lung slices were embedded in paraffin, sectioned and stained with H&E or periodic acid-Schiff (PAS). Histology was evaluated using an Olympus DP-25 digital camera, connected to a BX-51 (Olympus) microscope using 40- and 100-fold magnifications (Olympus cell A software). The area of mucin-containing goblet cells (GC), was quantified as previously described<sup>53</sup>, using systematic uniform random sampling<sup>54, 55</sup>. Airway responsiveness to methacholine (MCh) were obtained using invasive lung function assessments (FinePointe RC units, Data Sciences International) as previously described<sup>53</sup>.

### **Imiquimod (IMQ) psoriasis model.**

Wild-type twelve weeks old C57BL/6J male mice (Jackson Laboratories) were back-skin shaved and treated with hair removal cream (Nair). Application of 75mg IMQ (Aldara 5% IMQ) or control cream (Vaseline cream) was done daily (day 1– 5) on back-skin (IMQ receiving groups: IMQ group ( $n=10$ ) and MAB-mR3 group ( $n=9$ )/ control cream receiving group: vehicle group ( $n=3$ )). IP injections were given every other day (day 1,3 and 5). The vehicle and untreated IMQ group received mouse IgG control (20mg/kg, MAB Discovery). The IMQ treatment group received MAB-mR3 (20mg/kg, MAB Discovery). Ears were concurrently applied with control cream on left ear (all mice; 5mg Vaseline cream) and group appropriate stimuli cream on right ear (Vehicle group: 5mg Vaseline cream, IMQ and MAB-mR3 groups; 5mg IMQ cream).

Body weight and erythema development was monitored daily. Mice were euthanized day 6, where left and right ear thickness was measured using an engineer's micrometer (Mitutoyo). Whole blood cell counts were assessed using a HemaTrue analyzer (HESKA). Pictures of back-skin were visually scored (erythema and scaling, score 0 (no response) to 4 (maximum affected)) by 6 blinded people. RNA was isolated from skin puncture biopsies. Trizol (4°C, Invitrogen) and a rotor stator homogenizer were used to lyse samples. RNA was extracted from lysates using RNeasy Mini spin columns (Qiagen) following manufactures protocol. cDNA was produced from 0.8 µg RNA (NanoDrop) (High Capacity cDNA Reverse Transcription Kit (Applied Biosystems)). 50ng cDNA was used in a 20 µL real time qPCR reaction using SYBR Green master mix (Applied Biosystems) and 0.1 µM of either IL-36α,

IL-36 $\beta$ , IL-36 $\gamma$ , IL-17A, IL-17F or IL-22 primers. The qPCRs were run on a Bio-Rad CFX96 Real-time PCR Platform. GAPDH was used as reference gene, and ratios calculated using the Pfaffl method including analyzed primer efficiencies. We used the following primer sequences for mouse IL-36 $\alpha$  (Forward: 5'-ATCTGGACACTCTTGAGACG-3', reverse: 3'-GAGAGGCTTTTACAGGTTCC-5'), mouse IL-36 $\beta$  (Forward: 5'-CACTATGCATGGATCCTCAC-3', reverse: 3'-TGTCTCTACATGCTATCAAGC-5'), mouse IL-36 $\gamma$  (Forward: 5'-ATGGACACCCTACTTTGCTG-3', reverse: 5'-CAGGGTGGTGGTACAAATC-3'), mouse IL-17A (Forward: 5'-TCCAGAAGGCCCTCAGACTA-3', reverse: 3'-TCAGGACCAGGATCTCTTGC-5'), mouse IL-17F (Forward: 5'-CCATTCTGAGGGAGGTAGCA-3', reverse: 3'-GGGGTCTCGAGTGATGTTGT-5'), mouse IL-22 (Forward: 5'-TCATCGGGGAGAACTGTTC-3', reverse: 3'-TCTGGATGTTCTGGTTCGTCA-5') and mouse GAPDH (Forward: 5'-TGCACCACCAACTGCTTAGC-3', reverse: 3'-GGCATGGACTGTGGTCATGAG-5').

Myeloperoxidase (MPO) levels were measured in a freshly obtained skin biopsy, homogenized in 1% Triton-X 100 containing collagenase I and protease inhibitor (Complete Mini tablet, Roche) using a rotor stator homogenizer. The lysate was spun at 12,000g (4°C, 20 min.) and supernatants were used for cytokine measurement by ELISA and measurements of protein levels by Bradford assay (BioRad), following manufactures protocol. MPO were normalized to total protein in the sample.

### Common procedures, background information and statistical analysis.

Cytokine and soluble receptor concentrations were measured according to protocol using Duoset ELISA (R&D Systems) or multiplex assays (Quansys Biosciences). PBMCs for stimulations were freshly isolated (Histopaque-1077, Sigma Aldrich) using heparin containing tubes and washed 3 times with 0.9% saline before use. Cell lines tested mycoplasma free before use. PBMCs were obtained from healthy donors after obtaining informed consent. The study was approved by the Colorado Multiple Institutional Review Board (COMIRB). All in vivo mouse models were approved by the University of Colorado Denver Animal Care and Use Committee or the Animal Research Ethics Board of the Ministry of Environment (Kiel, Germany).

Cell line IC50 values were calculated using an incorporated [Inhibitor] vs. response function in GraphPad Prism. Comparison between IC50 values was done using the extra-sum-of-squares F test. Binding affinity for cell lines was calculated using a Binding-kinetics function in Graphpad Prism assuming complete specific binding. The impact of inhibitors on cell lines, PBMCs, whole-blood cultures and MLRs were evaluated using either a paired *t*-test (two-sided) or a Wilcoxon signed-rank test, as appropriate. Multiple comparisons were evaluated using Holm-Sidak's multiple comparisons test. Differences between groups in vivo were tested using Mann-Whitney *U*-test or Student's *t*-test, as appropriate. Two-tailed *p*-values  $\leq 0.05$  were considered significant. GraphPad Prism v.7 (GraphPad software) was used for statistical analysis and graphical presentations. For further information see the manuscript associated Life Sciences Reporting Summary.

## Data availability

The data that support the findings of this study are available upon request to the corresponding author.

## Supplementary Material

Refer to Web version on PubMed Central for supplementary material.

## Acknowledgements

We thank J. Domenico and M. Wade for their technical assistance, and S.H. Kim (Laboratory of Cytokine Immunology, Konkuk University, Republic Korea) for providing cell lines. We thank the OLAR Vivarium, the ClinImmune Flow Core Facility and the Histology Shared Resource Center funded by the University of Colorado Cancer Center NIH Grant (P30CA046934) at the University of Colorado Anschutz Medical Campus. We also thank the University of Colorado School of Medicine Biological Mass Spectrometry Facility for analyzing IP samples. J.F.H. was supported by the Oticon Foundation, Lundbeck Foundation, Knud Højgaard Foundation and the Interleukin Foundation. M.L.V.K and B.J.S. was supported by the Interleukin Foundation. A.S.M. is funded by NIH grants HL126736, ES025534 and HL135872–01. C.A.D. is funded by NIH Grant AI-15614.

## References

1. Kopf M, Bachmann MF & Marsland BJ Averting inflammation by targeting the cytokine environment. *Nature reviews. Drug discovery* 9, 703–718 (2010). [PubMed: 20811382]
2. Lappalainen U, Whitsett JA, Wert SE, Tichelaar JW & Bry K Interleukin-1beta causes pulmonary inflammation, emphysema, and airway remodeling in the adult murine lung. *Am J Respir Cell Mol Biol* 32, 311–318 (2005). [PubMed: 15668323]
3. Prefontaine D et al. Increased expression of IL-33 in severe asthma: evidence of expression by airway smooth muscle cells. *J Immunol* 183, 5094–5103 (2009). [PubMed: 19801525]
4. Towne JE & Sims JE IL-36 in psoriasis. *Curr Opin Pharmacol* 12, 486–490 (2012). [PubMed: 22398321]
5. Tortola L et al. Psoriasiform dermatitis is driven by IL-36-mediated DC-keratinocyte crosstalk. *J Clin Invest* 122, 3965–3976 (2012). [PubMed: 23064362]
6. Garlanda C, Dinarello CA & Mantovani A The interleukin-1 family: back to the future. *Immunity* 39, 1003–1018 (2013). [PubMed: 24332029]
7. Boraschi D & Tagliabue A The interleukin-1 receptor family. *Semin Immunol* 25, 394–407 (2013). [PubMed: 24246227]
8. Wesche H et al. The interleukin-1 receptor accessory protein (IL-1RAcP) is essential for IL-1-induced activation of interleukin-1 receptor-associated kinase (IRAK) and stress-activated protein kinases (SAP kinases). *J Biol Chem* 272, 7727–7731 (1997). [PubMed: 9065432]
9. Korherr C, Hofmeister R, Wesche H & Falk W A critical role for interleukin-1 receptor accessory protein in interleukin-1 signaling. *Eur J Immunol* 27, 262–267 (1997). [PubMed: 9022028]
10. Hezareh M, Hessel AJ, Jensen RC, van de Winkel JG & Parren PW Effector function activities of a panel of mutants of a broadly neutralizing antibody against human immunodeficiency virus type 1. *Journal of virology* 75, 12161–12168 (2001). [PubMed: 11711607]
11. Leabman MK et al. Effects of altered FcγR binding on antibody pharmacokinetics in cynomolgus monkeys. *MAbs* 5, 896–903 (2013). [PubMed: 24492343]
12. Hansel TT, Kropshofer H, Singer T, Mitchell JA & George AJ The safety and side effects of monoclonal antibodies. *Nature reviews. Drug discovery* 9, 325–338 (2010). [PubMed: 20305665]
13. Lee DW et al. Current concepts in the diagnosis and management of cytokine release syndrome. *Blood* 124, 188–195 (2014). [PubMed: 24876563]
14. Smith DE et al. The soluble form of IL-1 receptor accessory protein enhances the ability of soluble type II IL-1 receptor to inhibit IL-1 action. *Immunity* 18, 87–96 (2003). [PubMed: 12530978]

15. Ter Horst R et al. Host and Environmental Factors Influencing Individual Human Cytokine Responses. *Cell* 167, 1111–1124 e1113 (2016). [PubMed: 27814508]
16. Gantner BN, Simmons RM, Canavera SJ, Akira S & Underhill DM Collaborative induction of inflammatory responses by dectin-1 and Toll-like receptor 2. *The Journal of experimental medicine* 197, 1107–1117 (2003). [PubMed: 12719479]
17. Gow NA et al. Immune recognition of *Candida albicans* beta-glucan by dectin-1. *The Journal of infectious diseases* 196, 1565–1571 (2007). [PubMed: 18008237]
18. Martinon F, Petrilli V, Mayor A, Tardivel A & Tschopp J Gout-associated uric acid crystals activate the NALP3 inflammasome. *Nature* 440, 237–241 (2006). [PubMed: 16407889]
19. Busso N & So A Mechanisms of inflammation in gout. *Arthritis Res Ther* 12, 206 (2010). [PubMed: 20441605]
20. Joosten LA et al. Engagement of fatty acids with Toll-like receptor 2 drives interleukin-1beta production via the ASC/caspase 1 pathway in monosodium urate monohydrate crystal-induced gouty arthritis. *Arthritis Rheum* 62, 3237–3248 (2010). [PubMed: 20662061]
21. Pham CT Neutrophil serine proteases: specific regulators of inflammation. *Nat Rev Immunol* 6, 541–550 (2006). [PubMed: 16799473]
22. Kakimoto K, Matsukawa A, Yoshinaga M & Nakamura H Suppressive effect of a neutrophil elastase inhibitor on the development of collagen-induced arthritis. *Cell Immunol* 165, 26–32 (1995). [PubMed: 7671322]
23. Lee HY et al. Blockade of IL-33/ST2 ameliorates airway inflammation in a murine model of allergic asthma. *Exp Lung Res* 40, 66–76 (2014). [PubMed: 24446582]
24. Marrakchi S et al. Interleukin-36-receptor antagonist deficiency and generalized pustular psoriasis. *N Engl J Med* 365, 620–628 (2011). [PubMed: 21848462]
25. Rossi-Semerano L et al. First clinical description of an infant with interleukin-36-receptor antagonist deficiency successfully treated with anakinra. *Pediatrics* 132, e1043–1047 (2013). [PubMed: 24019411]
26. Flutter B & Nestle FO TLRs to cytokines: mechanistic insights from the imiquimod mouse model of psoriasis. *Eur J Immunol* 43, 3138–3146 (2013). [PubMed: 24254490]
27. Libby P Inflammation in atherosclerosis. *Arterioscler Thromb Vasc Biol* 32, 2045–2051 (2012). [PubMed: 22895665]
28. Grivennikov SI, Greten FR & Karin M Immunity, inflammation, and cancer. *Cell* 140, 883–899 (2010). [PubMed: 20303878]
29. Ramanan VK et al. GWAS of longitudinal amyloid accumulation on 18F-florbetapir PET in Alzheimer's disease implicates microglial activation gene IL1RAP. *Brain* 138, 3076–3088 (2015). [PubMed: 26268530]
30. Jaras M et al. Isolation and killing of candidate chronic myeloid leukemia stem cells by antibody targeting of IL-1 receptor accessory protein. *Proc Natl Acad Sci U S A* 107, 16280–16285 (2010). [PubMed: 20805474]
31. Ridker PM et al. Antiinflammatory Therapy with Canakinumab for Atherosclerotic Disease. *N Engl J Med* 377, 1119–1131 (2017). [PubMed: 28845751]
32. Ridker PM et al. Effect of interleukin-1beta inhibition with canakinumab on incident lung cancer in patients with atherosclerosis: exploratory results from a randomised, double-blind, placebo-controlled trial. *Lancet* 390, 1833–1842 (2017). [PubMed: 28855077]
33. Bertheloot D & Latz E HMGB1, IL-1alpha, IL-33 and S100 proteins: dual-function alarmins. *Cell Mol Immunol* 14, 43–64 (2017). [PubMed: 27569562]
34. Hueber AJ et al. IL-33 induces skin inflammation with mast cell and neutrophil activation. *Eur J Immunol* 41, 2229–2237 (2011). [PubMed: 21674479]
35. Enoksson M et al. Intraperitoneal influx of neutrophils in response to IL-33 is mast cell-dependent. *Blood* 121, 530–536 (2013). [PubMed: 23093619]
36. Afonina IS, Muller C, Martin SJ & Beyaert R Proteolytic Processing of Interleukin-1 Family Cytokines: Variations on a Common Theme. *Immunity* 42, 991–1004 (2015). [PubMed: 26084020]

37. Guma M et al. Caspase 1-independent activation of interleukin-1beta in neutrophil-predominant inflammation. *Arthritis Rheum* 60, 3642–3650 (2009). [PubMed: 19950258]
38. Nakae S et al. IL-1 is required for allergen-specific Th2 cell activation and the development of airway hypersensitivity response. *Int Immunol* 15, 483–490 (2003). [PubMed: 12663678]
39. Rabeony H et al. IMQ-induced skin inflammation in mice is dependent on IL-1R1 and MyD88 signaling but independent of the NLRP3 inflammasome. *Eur J Immunol* 45, 2847–2857 (2015). [PubMed: 26147228]
40. Possa SS, Leick EA, Prado CM, Martins MA & Tiberio IF Eosinophilic inflammation in allergic asthma. *Front Pharmacol* 4, 46 (2013). [PubMed: 23616768]
41. Tanabe T, Shimokawaji T, Kanoh S & Rubin BK IL-33 stimulates CXCL8/IL-8 secretion in goblet cells but not normally differentiated airway cells. *Clin Exp Allergy* 44, 540–552 (2014). [PubMed: 24479526]
42. Alvarez P & Jensen LE Imiquimod Treatment Causes Systemic Disease in Mice Resembling Generalized Pustular Psoriasis in an IL-1 and IL-36 Dependent Manner. *Mediators Inflamm* 2016, 6756138 (2016). [PubMed: 28057979]
43. Sticherling M, Sautier W, Schroder JM & Christophers E Interleukin-8 plays its role at local level in psoriasis vulgaris. *Acta Derm Venereol* 79, 4–8 (1999). [PubMed: 10086849]
44. Hawkes JE, Chan TC & Krueger JG Psoriasis pathogenesis and the development of novel targeted immune therapies. *J Allergy Clin Immunol* 140, 645–653 (2017). [PubMed: 28887948]
45. Mashiko S et al. Human mast cells are major IL-22 producers in patients with psoriasis and atopic dermatitis. *J Allergy Clin Immunol* 136, 351–359 e351 (2015). [PubMed: 25792465]
46. Betz UA et al. Postnatally induced inactivation of gp130 in mice results in neurological, cardiac, hematopoietic, immunological, hepatic, and pulmonary defects. *The Journal of experimental medicine* 188, 1955–1965 (1998). [PubMed: 9815272]
47. Cao X et al. Defective lymphoid development in mice lacking expression of the common cytokine receptor gamma chain. *Immunity* 2, 223–238 (1995). [PubMed: 7697543]
48. Cullinan EB et al. IL-1 receptor accessory protein is an essential component of the IL-1 receptor. *J Immunol* 161, 5614–5620 (1998). [PubMed: 9820540]
49. Dyballa N & Metzger S Fast and sensitive colloidal coomassie G-250 staining for proteins in polyacrylamide gels. *J Vis Exp* (2009).
50. Moore HB et al. Hemolysis exacerbates hyperfibrinolysis, whereas plateletolysis shuts down fibrinolysis: evolving concepts of the spectrum of fibrinolysis in response to severe injury. *Shock* 43, 39–46 (2015). [PubMed: 25072794]
51. van de Veerdonk FL et al. Protective host defense against disseminated candidiasis is impaired in mice expressing human interleukin-37. *Front Microbiol* 5, 762 (2014). [PubMed: 25620965]
52. McKee AS, Mack DG, Crawford F & Fontenot AP MyD88 dependence of beryllium-induced dendritic cell trafficking and CD4(+) T-cell priming. *Mucosal Immunol* 8, 1237–1247 (2015). [PubMed: 25760420]
53. Lunding LP et al. Poly(inosinic-cytidylic) acid-triggered exacerbation of experimental asthma depends on IL-17A produced by NK cells. *J Immunol* 194, 5615–5625 (2015). [PubMed: 25972482]
54. Fehrenbach H et al. Ultrastructural pathology of the alveolar type II pneumocytes of human donor lungs. Electron microscopy, stereology, and microanalysis. *Virchows Arch* 432, 229–239 (1998). [PubMed: 9532002]
55. Mattfeldt T, Mall G, Gharehbaghi H & Moller P Estimation of surface area and length with the orientator. *J Microsc* 159, 301–317 (1990). [PubMed: 2243364]

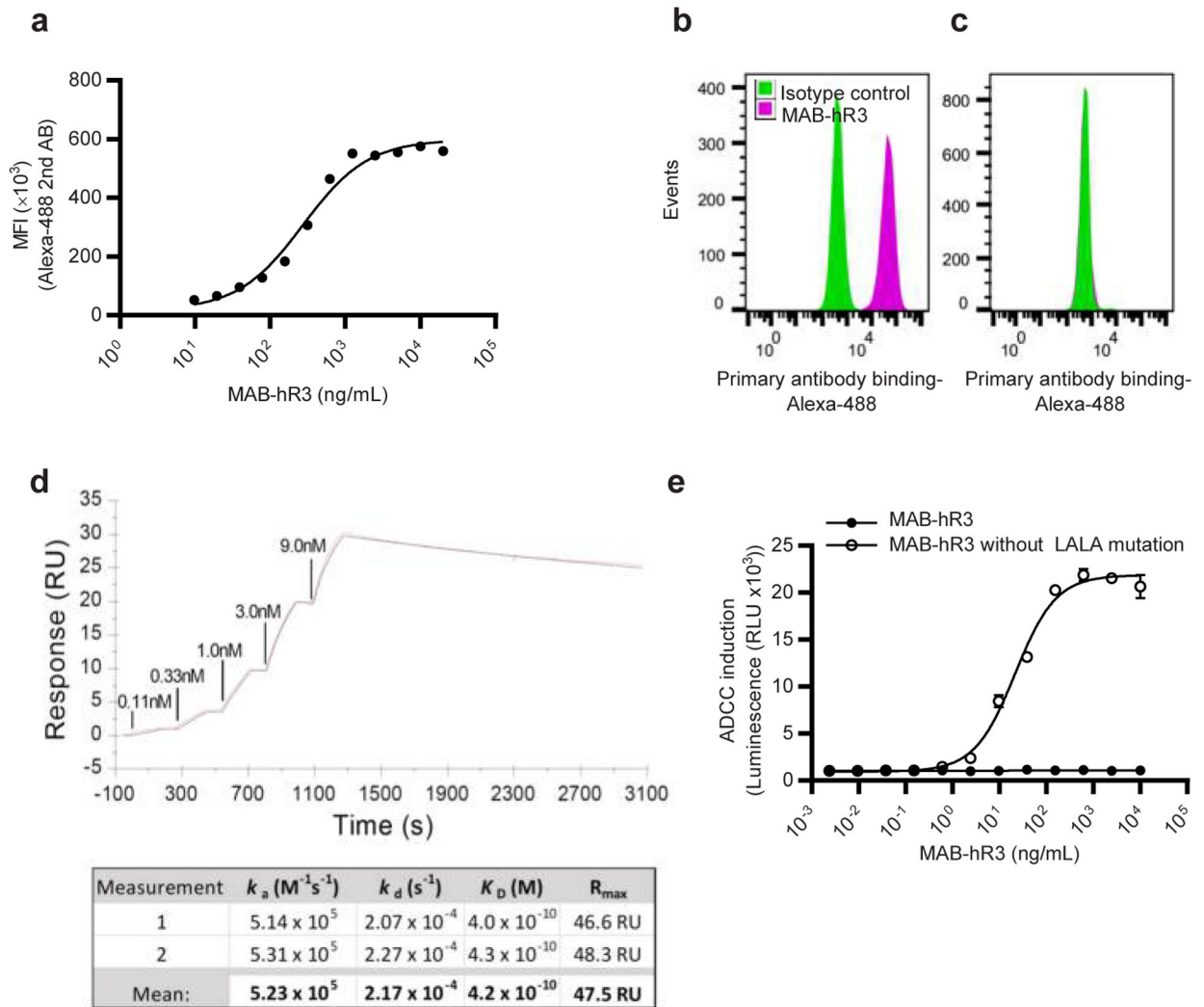


**Figure 1. MAB-hR3 binds dose-dependently and with high affinity to IL-1R3.**

(a) Dose-dependent binding of MAB-hR3 (using FACS analysis) to the IL-1R3 expressing human cell line SK-MEL-30 (represented as mean fluorescence intensity (MFI)). (b+c) FACS analysis of MAB-hR3 binding to IL-1R3 expressing human cell line SK-MEL-30 (-b) and the murine cell line NIH-3T3 (-c) (isotype control included). (d) MAB-hR3 kinetics analyzed using SPR (1 measurement depicted). Single-cycle kinetics were done using increasing concentrations of hIL-1R3 (0.111nM - 9nM). (e) The impact of the incorporated MAB-hR3 LALA mutation on binding to Fc $\gamma$ RIIIa as measured by NFAT reporter gene activation in an ADCC luciferase Reporter Bioassay (Jurkat effector cells). Data are from one representative experiment (a-d) confirmed once with similar results. Mean  $\pm$ SEM depicted from 4 technical replicates (e).

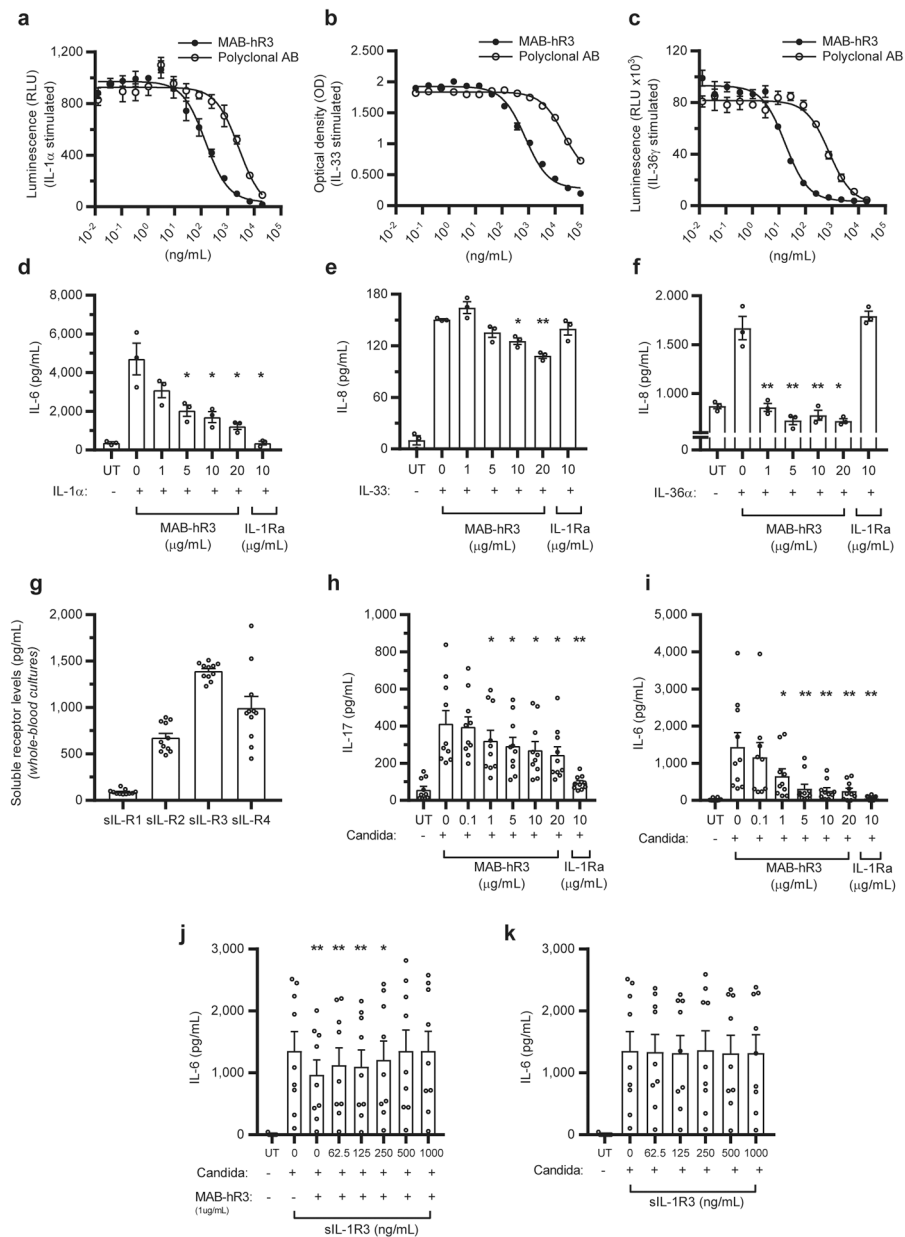


**Figure 2. MAB-hr3 inhibits IL-1R1, IL-1R4 and IL-1R6 signaling in vitro and is functional ex vivo.**

(a-c) Suppression of cytokine signaling by MAB-hr3 compared to polyclonal goat anti-IL-1R3. (-a) Inhibition of IL-1 $\alpha$  signaling in an A549 luciferase reporter cell line (NF- $\kappa$ B activation) (IC50: MAB-hr3=146ng/mL, polyclonal=2609ng/mL;  $p < 0.0001$ ). (-b) IL-33 signaling inhibition in an HEK293 SEAP reporter cell line (NF- $\kappa$ B/ AP-1 activation) (IC50: MAB-hr3=749ng/mL, polyclonal=20986ng/mL,  $p < 0.0001$ ). (-c) IL-36 $\gamma$  signaling inhibition in an HEK293/17 luciferase reporter cell line (NF- $\kappa$ B activation) (IC50: MAB-hr3=17.1ng/mL, polyclonal=769ng/mL,  $p < 0.0001$ ). (d-f) Comparison of cytokine production by MAB-hr3 to IL-1Ra (-d) IL-1 $\alpha$  induced IL-6 production in a human lung epithelial cell line (A549). (-e) IL-33 induced IL-8 production in a human mast cell line

(HMC-1). **(-f)** IL-36 $\alpha$  induced IL-8 production in a human keratinocytic cell line (HaCaT). **(g)** The levels of soluble receptors in whole-blood cultures after 24hrs of incubation in media **(h+i)** Heat-killed (hk.) *C. albicans* stimulation ( $0.5 \times 10^6$ /mL, 24hrs) of IL-17 and IL-6 production in whole-blood cultures. **(j)** Pre-incubation (14hrs) of MAB-hR3 (1 $\mu$ g/mL) with recombinant human soluble IL-1R3 (sIL-1R3) in increasing concentrations, before evaluating IL-6 production in hk. *C. albicans* stimulated whole blood. **(k)** The anti-inflammatory effect of various concentrations of sIL-1R3 alone on hk. *C. albicans* stimulated whole blood. UT; untreated. IL-1Ra; 10 $\mu$ g/mL= 578nM. MAB-hR3; 10 $\mu$ g/mL=69nM. Inhibitors compared to stimulation alone. \* $p < 0.05$ , \*\* $p < 0.01$  (Paired *t*-test, two-sided). Mean  $\pm$ SEM depicted. Data are from one representative experiment (a-c) confirmed once with similar results,  $n=3$  independent experiments (d-f),  $n=11$  (g),  $n=10$  (h,i) and  $n=9$  (j,k) donors.

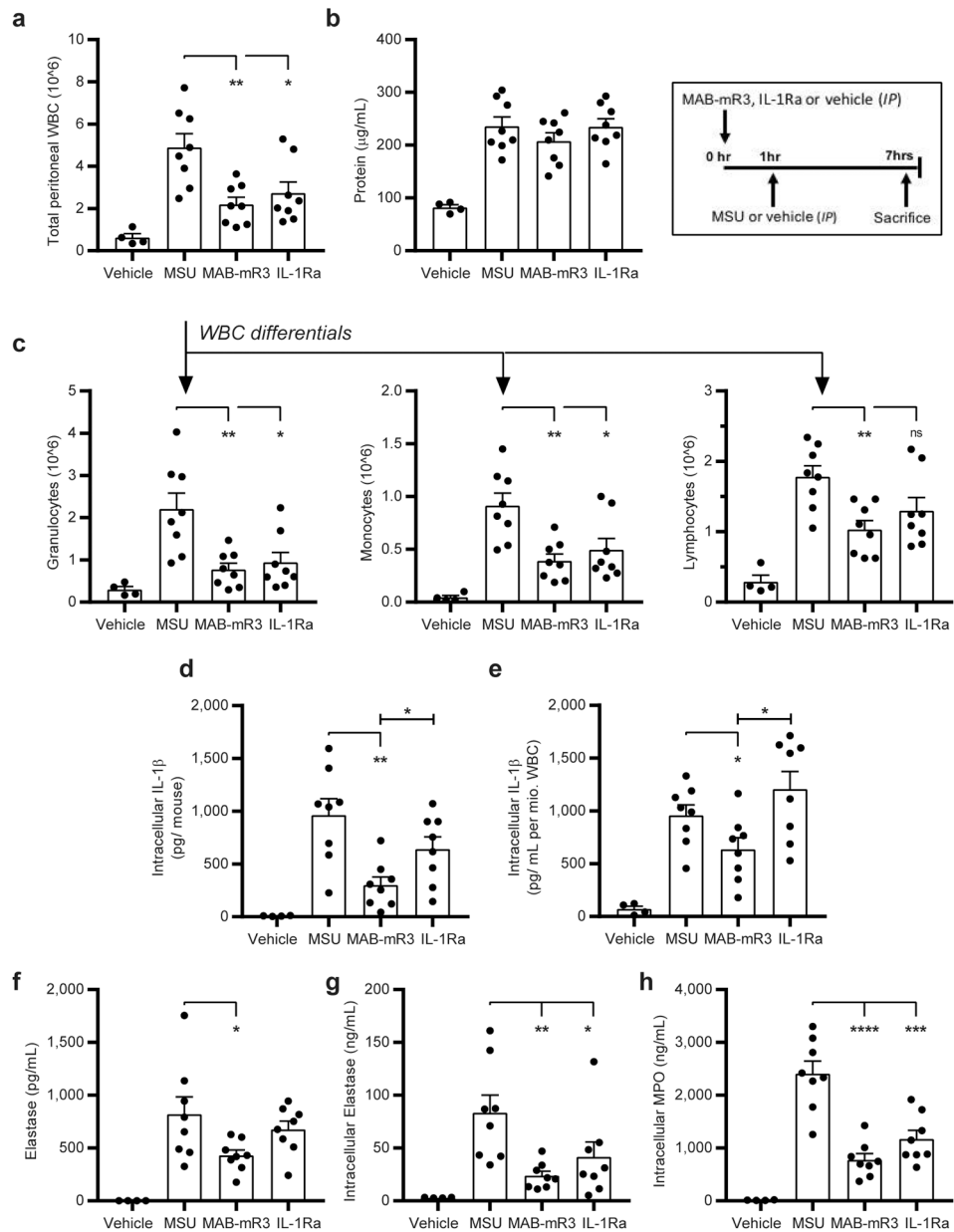


**Figure 3. MAB-mR3 reduces in vivo monosodium urate crystal (MSU) mediated peritonitis.** (a) Total white blood cell count (WBC) from the peritoneal cavity (IP fluid). (b) Protein concentration in IP fluid. (c) Differential cell counts from (a) total cell influx. (ns:  $p=0.07$ ) (d) Total levels per mouse of intracellular IL-1 $\beta$  in WBC from IP fluid. (e) Levels of intracellular IL-1 $\beta$  normalized per mio. WBC from IP fluid. (f) Levels of the neutrophil protease Elastase in IP fluid. (g) Total levels of intracellular Elastase in WBC from IP fluid. (h) Total levels of intracellular MPO in WBC from IP fluid. Vehicle group; vehicle+ vehicle ( $n=4$ ). MSU group; vehicle+ MSU ( $n=8$ ). MAB-mR3 group; MAB-mR3+ MSU ( $n=8$ ). IL-1Ra group; IL-1Ra+MSU ( $n=8$ ). Comparisons between inhibitor treated and MSU stimulated groups (a-h) and in-between treatment groups (d, e).

\*  $p < 0.05$ , \*\*  $p < 0.01$ , \*\*\*  $p < 0.001$ , \*\*\*\*  $p < 0.0001$  (Student's  $t$ -test, two sided), mean  $\pm$ SEM depicted.

Author Manuscript

Author Manuscript

Author Manuscript

Author Manuscript

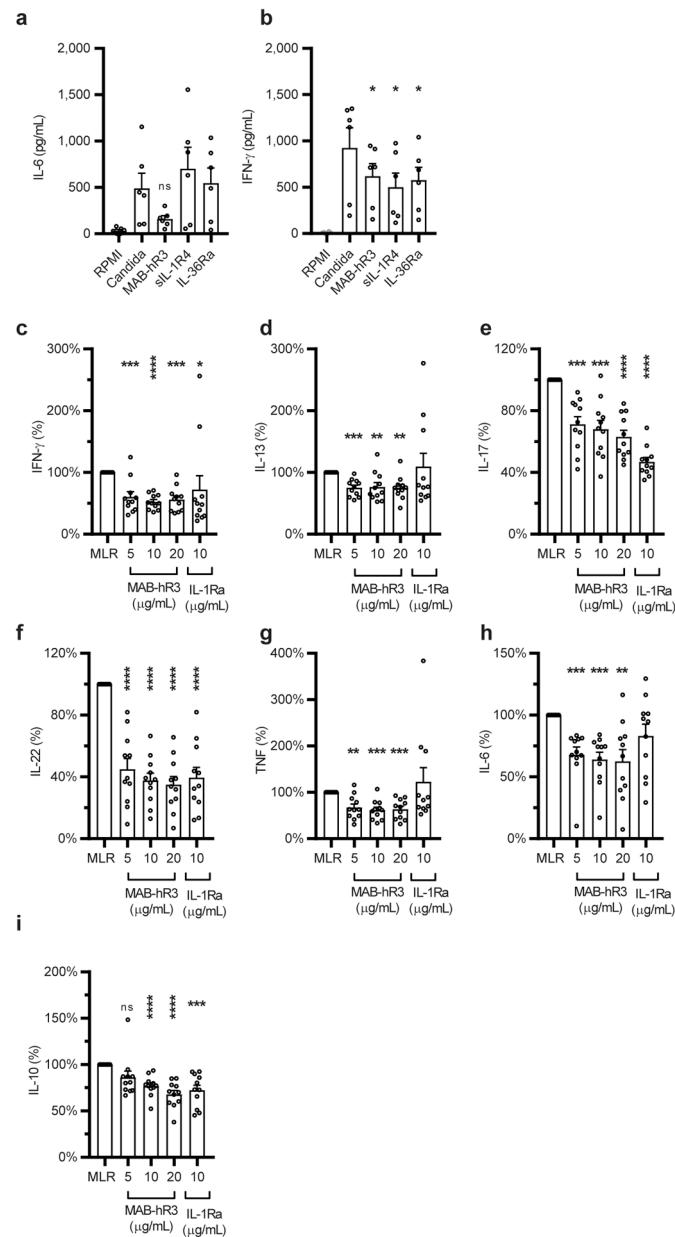


**Figure 4. IL-1R3 blockade results in a broader anti-inflammatory phenotype compared to primary pathway inhibition.**

(a+b) Inhibition of hk. *C. albicans* ( $0.5 \times 10^6$ /mL, 24hrs) induced IL-6 (a) or IFN- $\gamma$  (b) production in PBMCs, using equal concentrations MAB-hR3, sIL-1R4 and IL-36Ra (69nM) (ns:  $p=0.052$ ) (c-i) Percent change in cytokines measured in the supernatants of two-way MLRs (5-day culture). MLR range of IFN- $\gamma$  (1.9–10.7 ng/mL, IL-13 (312–1808 pg/mL), IL-17 (48.6–189 ng/mL), IL-22 (143–2696 pg/mL), TNF (168–1712 pg/mL), IL-6 (254–8361 pg/mL) and IL-10 (107–1302 pg/mL) (ns:  $p=0.07$ ). Inhibitors compared to stimulation or MLR alone. \* $p<0.05$ , \*\* $p<0.01$ , \*\*\* $p<0.001$ , \*\*\*\* $p<0.0001$  (Paired  $t$ -test, two-sided), mean +SEM depicted. Data are from  $n=6$  donors (a+b) and  $n=11$  independent experiments (MLR, c-i). IL-1Ra; 10 $\mu$ g/mL= 578nM. MAB-hR3; 10 $\mu$ g/mL=69nM.

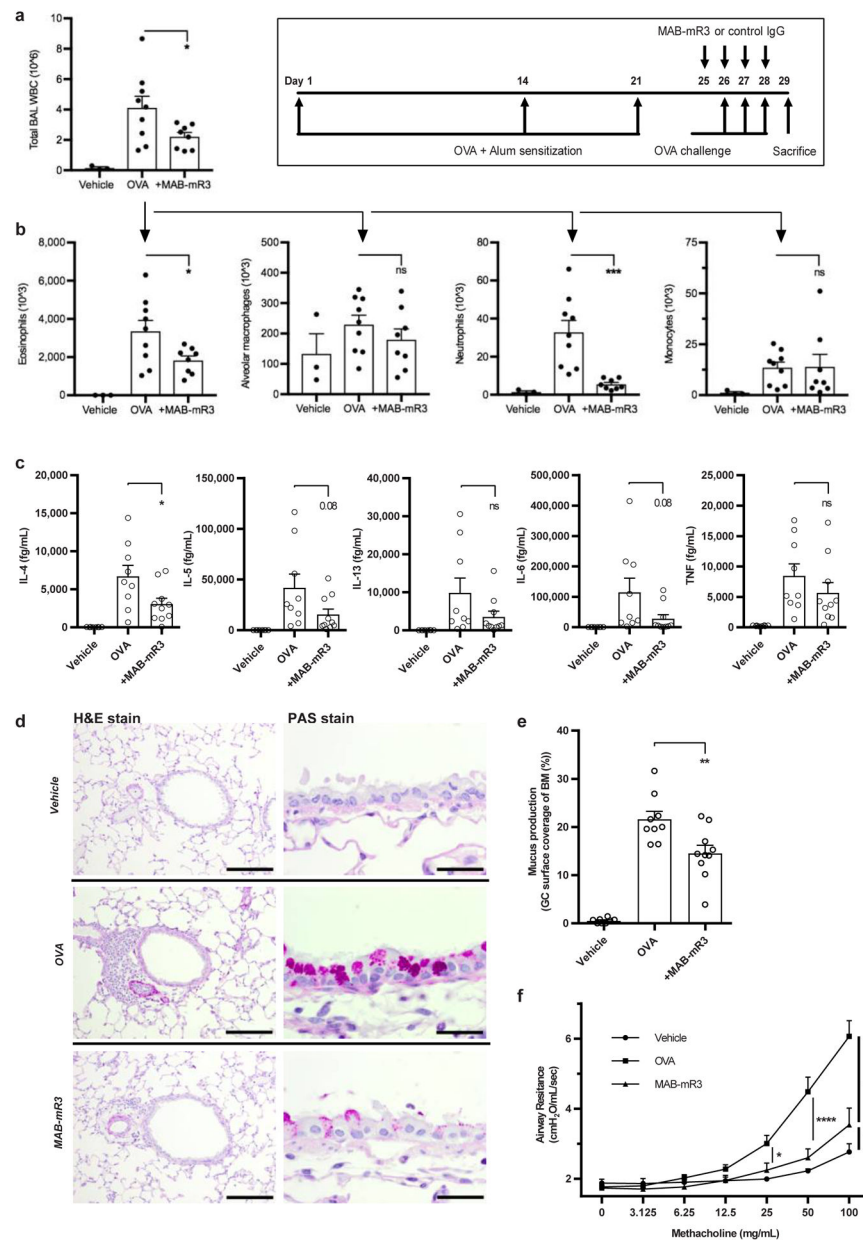


**Figure 5. MAB-mR3 decreases ovalbumin-induced allergic airway inflammation.**

**(a+b)** Mice challenged by intranasal OVA (Exp.1).  $n=4$  (vehicle),  $n=9$  (OVA) and  $n=8$  (+MAB-mR3). **(a)** Total WBC from BAL fluid. **(b)** Flow defined cell differentials from (a). **(c-f)** Mice challenged by OVA aerosols (Exp. 2).  $n=8$  (vehicle),  $n=9$  (OVA) and  $n=10$  (+MAB-mR3) **(c)** Cytokine measurements on BAL fluid. **(d)** Cross-sections from each interventional group using H&E (Scale bar: 100  $\mu\text{m}$ ) and PAS (Scale bar: 20  $\mu\text{m}$ ) stained lung tissue, completed for each mouse with similar results. **(e)** Area of airway epithelial basal membrane (BM) covered by goblet cells (GC) (%). **(f)** Airway resistance to increasing concentrations of methacholine. (a-c, e), from  $n=6$  (vehicle),  $n=9$  (OVA) and  $n=9$  (+MAB-mR3). Comparisons between MAB-mR3 treated mice and OVA alone (Student's *t*-test, two-

sided). (f) Comparisons between all groups at each concentration (Holm-Sidak's Multiple comparisons test).

\*  $p < 0.05$ , \*\*  $p < 0.01$ , \*\*\*  $p < 0.001$ , ns; non-significant. Mean +SEM depicted.

Author Manuscript

Author Manuscript

Author Manuscript

Author Manuscript

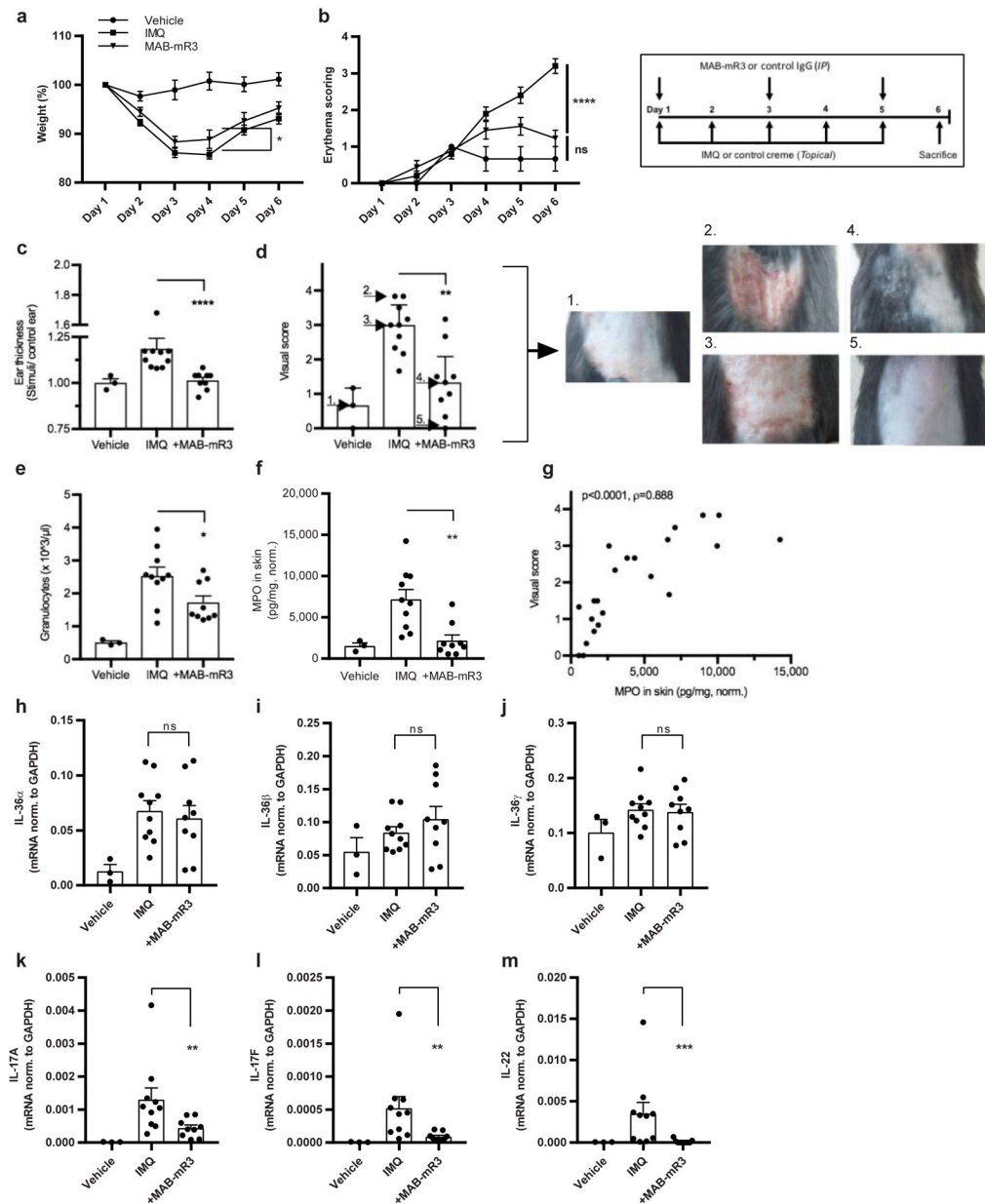


**Figure 6. Improvement of imiquimod- induced psoriasis in vivo using MAB-mR3.** (a+b) Daily monitoring of (a) weight (percentage) and (b) erythema (scores: 0; unaffected – 4; maximum affected (unblinded)) throughout the experiment. (c) Fold change in ear thickness between IMQ and control cream applied ears on day 6. (d) Visual scoring by  $n=6$  blinded people at end of study (0; unaffected – 4; maximum affected (erythema and scaling)), arrow and number indicate depicted mice. (e) Granulocyte concentrations in whole blood. (f) MPO concentration in skin, normalized (norm.) per mg of protein. (g) Spearman correlation between data from (d) and (f). (h-m) mRNA expression of cytokines in back skin, normalized (norm.) to GAPDH expression. Data from  $n=3$  (vehicle),  $n=10$  (IMQ) and  $n=9$  (+MAB-mR3). (a+b) Holm-Sidak's Multiple comparisons test (all groups compared). (c-

m) Comparisons between inhibitor treated and IMQ stimulated groups. (c, k-m) Mann-Whitney *U*-test, (d-f, h-j) Student's *t*-test).

\*  $p < 0.05$ , \*\*  $p < 0.01$ , \*\*\*  $p < 0.001$ , \*\*\*\*  $p < 0.0001$ , ns; non-significant. Mean  $\pm$  SEM depicted.

Author Manuscript

Author Manuscript

Author Manuscript

Author Manuscript

**Table 1:**  
**Local and systemic inflammation in MSU mediated peritonitis.**

Cytokine and chemokine concentrations locally (IP fluid) and systemically. WB; lysed whole blood, norm.; normalized per mg of protein in spleen. Vehicle group; vehicle+vehicle ( $n=4$ ). MSU group; vehicle+MSU ( $n=8$ ). MAB-mR3 group; MAB-mR3+ MSU ( $n=8$ ). IL-1Ra group; IL-1Ra+MSU ( $n=8$ ). Comparisons between inhibitor treated and MSU stimulated groups. Student's  $t$ -test (two-sided) with mean  $\pm$ SEM, except: G-CSF, CXCL-1 in WB and CXCL-1 in spleen; Mann-Whitney  $U$ -test with median and IQR.

IP fluid	Vehicle (n=4)	MSU stimulated (n=8)	MAB-mR3 (n=8)	IL-1Ra (n=8)
<b>IL-6 (pg/mL)</b>	Below detection	65.0 $\pm$ 14.9	19.8 $\pm$ 5.8 ( <b>p=0.014</b> )	36.9 $\pm$ 14.4 (p=0.164)
<b>G-CSF (pg/mL)</b>	5.0 (2.8–5.5)	77.7 (53.6–97.3)	6.6 (4.9–33.0) ( <b>p=0.015</b> )	8.6 (7.5–17.8) ( <b>p=0.005</b> )
<b>CXCL-1 (pg/mL)</b>	2.3 $\pm$ 0.5	82.7 $\pm$ 15.9	38.4 $\pm$ 11.6 ( <b>p=0.041</b> )	84.3. $\pm$ 31.9 (p=0.965)
<b>CCL-2 (pg/mL)</b>	Below detection	62.5 $\pm$ 11.9	26.2 $\pm$ 3.6 ( <b>p=0.011</b> )	74.2 $\pm$ 14.5 (p=0.545)
<b>CCL-3 (pg/mL)</b>	1.2 $\pm$ 0.1	4.9 $\pm$ 0.8	3.6 $\pm$ 0.5 (p=0.161)	5.7 $\pm$ 0.9 (p=0.545)
Systemic	Vehicle (n=4)	MSU stimulated (n=8)	MAB-mR3 (n=8)	IL-1Ra (n=8)
<b>IL-6 (pg/mL), plasma</b>	5.0 $\pm$ 3.4	69.8 $\pm$ 19.4	22.7 $\pm$ 5.7 ( <b>p=0.011</b> )	29.5 $\pm$ 8.5 ( <b>p=0.078</b> )
<b>G-CSF (pg/mL), plasma</b>	294 $\pm$ 28.4	6245 $\pm$ 1055	3544 $\pm$ 2743 ( <b>p=0.010</b> )	1157 $\pm$ 639 ( <b>p=0.003</b> )
<b>CXCL-1 (pg/mL), WB</b>	272 (243–719)	2525 (2178–2730)	1366 (811–1889) (p=0.065)	2269 (1511–3213) (p=0.959)
<b>MPO (ng norm.), spleen</b>	42.5 $\pm$ 7.6	145 $\pm$ 9.7	89.3 $\pm$ 11.4 ( <b>p=0.002</b> )	106 $\pm$ 9.7 ( <b>p=0.013</b> )
<b>CXCL-1 (pg norm.), spleen</b>	16.2 (13.3–39.3)	189 (161–205)	72.5 (49.6–140) ( <b>p=0.010</b> )	157 (95.3–238) (p=0.645)